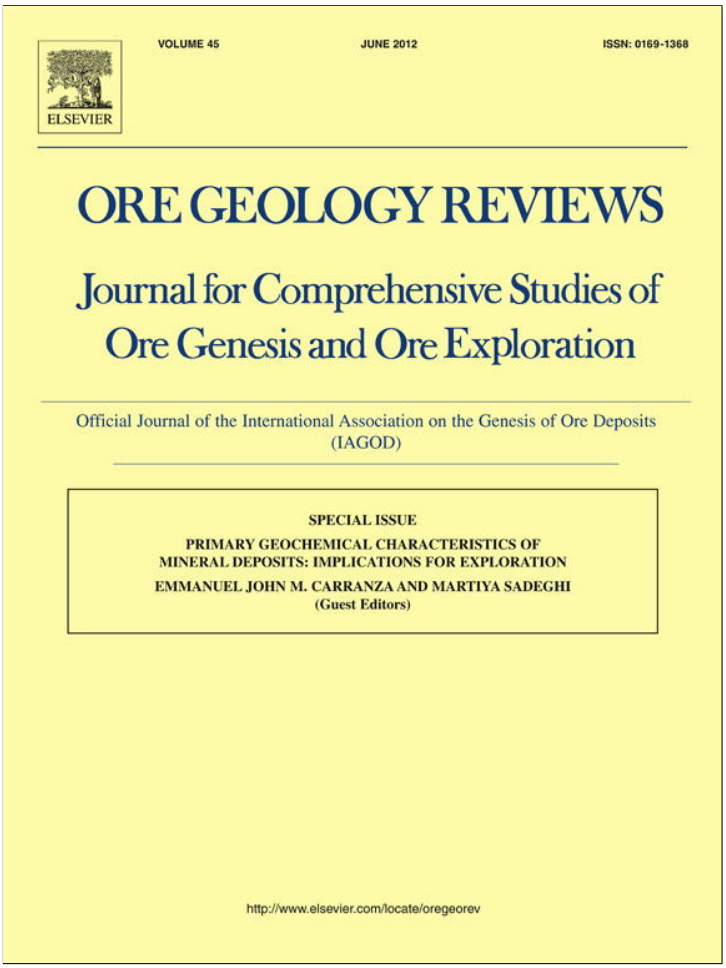

Ore Geology Reviews 45 (2012) 16–32

Contents lists available at SciVerse ScienceDirect

Ore Geology Reviews

journal homepage: www.elsevier.com/locate/oregeorev

Post-orogenic, Carboniferous granite-hosted Sn–W mineralization in the Sierras Pampeanas Orogen, Northwestern Argentina

A.S. Fogliata [a,b,*], M.A. Báez [b], S.G. Hagemann [c], J.O. Santos [c], F. Sardi [b]

[a] Fundación Miguel Lillo & University of Tucumán, Miguel Lillo 251, 4000-San Miguel de Tucumán, Tucumán, Argentina
[b] Facultad de Ciencias Naturales, University of Tucumán, Miguel Lillo 205, 4000-San Miguel de Tucumán, Tucumán, Argentina
[c] University of Western Australia, School of Earth and Environment, Centre for Exploration Targeting, Nedlands, W.A. 6009, Australia

ARTICLE INFO

Article history:
Received 20 October 2010
Received in revised form 16 December 2011
Accepted 21 December 2011
Available online 8 January 2012

Keywords:
Sn–W mineralization
Sierras Pampeanas
Granites
Argentina

ABSTRACT

The Sierras Pampeanas orogen, in northwestern Argentina, hosts significant Sn–W mineralization in a variety of mostly epizonal granite stocks emplaced in variably metamorphosed country rocks. The San Blas, Huaco and El Durazno granite stocks in the Sierra de Velasco, the La Quebrada granite in the Sierra de Mazán, the Cerro Colorado granite in the Cerro Negro, and the Los Mudaderos and Sauce Guacho granite stocks in the Sierra de Ancasti, are largely peraluminous (ASI between 1.05 and 1.38) and represent S-type granites, are strongly fractionated (i.e., high Rb–Sr ratio), have a low oxidation state (low Fe_2O_3/Fe_2O_3 ratio) and are geotectonically linked to syncollisional magmatism. The U–Pb SHRIMP analyses on zircons from the Cerro Colorado and La Quebrada granites, located in the Cerro Negro and Sierra de Mazán, respectively, revealed ages from Lower Ordovician (Tremadocian) to Carboniferous. All granites display elevated LREE values, low HREE values and negative Eu anomalies. With regards to total REE values, two groups of granite stocks can be recognized. The granites with lower REE contents are highly evolved granites and are related to Sn–W mineralization. The mineralized granites display higher values of Sn, W and Rb, and lower values of Sr and Ba compared to barren granites. These trace element characteristics appear to be diagnostic for Sn–W mineralized granite stocks in the western Sierras Pampeanas. The western Sierras Pampeanas contains locally geochemically evolved Carboniferous granites, which are interpreted to be the main control of significant Sn–W mineralization. The Carboniferous age of western Sierras Pampeanas Sn–W mineralization sets it apart from the Triassic age of the Sn–W mineralization in the Eastern Tin belt of Bolivia.

1. Introduction

The relationship between granitic rocks and Sn–W mineralization is well known and numerous authors have referred to evolved granites that are associated with this type of mineralization (Kempe and Wolf, 2006; Linnen, 1998; Olade, 1980; Srivastava and Sinha, 1997; Tauson and Kozlov, 1973; Vriend et al., 1985; Xie et al., 2009). This type of mineralization is particularly related to S- and A-type granite intrusions, which are emplaced at shallow crustal levels, associated with peralkaline to peraluminous magmas (Tischendorf, 1977). These granites are enriched in F, B, Li and Rb, and contain typical minerals such as fluorite, topaz and Li-bearing mica (Pollard et al., 1987).

In Argentina, Sn–W mineralization has been described from various Carboniferous granites in the Sierras Pampeanas orogen (Fig. 1) such as Sierra de Velasco (Báez, 2006), Sierra de Mazán (Fogliata and Báez, 2008) and Sierra de Fiambalá (Fogliata et al., 2008). Despite these numerous and detailed descriptions of Sn–W deposits and old workings, there is a distinctive dearth in geochemical characterization, particularly rare earth element (REE) analyses, of granites hosting Sn–W mineralization.

The objective of this paper is the geochemical characterization and U–Pb isotopic age dating of the granites associated with Sn–W mineralization in the western Sierras Pampeanas in order to constrain the: (1) geochemical trends; (2) crystallization age; (3) fertility with respect to Sn and W mineralization; and (4) whole rock major element, trace element and REE characteristics (pathfinder elements) for fertile Sn–W granitoid stocks. In combination, the petrological–geochemical characterization and age dating of the granites provide a geological framework of the Sn–W mineral system in the Sierras Pampeanas, which can be used for exploration of these metals.

2. Regional geological setting

The Sierras de Velasco, Cerro Negro and Ancasti are located in the Sierras Pampeanas (Fig. 1), which are defined by González Bonorino (1950) as mountain blocks that are elevated over reverse faults. They are located in the central batholith zone (Toselli and Rossi de Toselli, 1986), which corresponds to the western Sierras Pampeanas

* Corresponding author at: Área Geología - Fundación Miguel Lillo, Miguel Lillo 251 - 4000 San miguel de Tucumán, Tucumán, Argentina.
E-mail addresses: anafogliata@yahoo.com.ar (A.S. Fogliata), steffen.hagemann@uwa.edu.au (S.G. Hagemann).

0169-1368/$ – see front matter © 2012 Elsevier B.V. All rights reserved.
doi:10.1016/j.oregeorev.2011.12.001

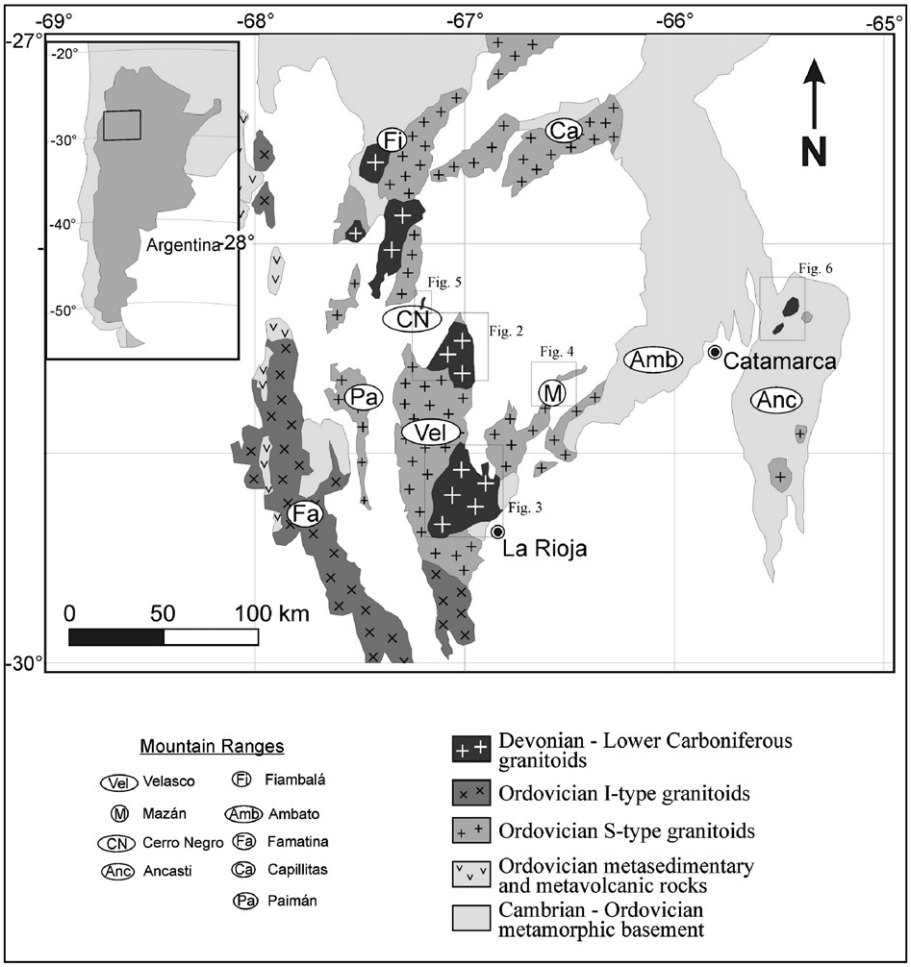

Fig. 1. Regional geological map of the western Sierras Pampeanas showing locations of major mountain ranges and granitoid. Modified after Grosse et al. (2009).

(Ramos, 1999) and are characterized by a significant volume of granitic intrusions and metamorphic rocks. The basement of the western Sierras Pampenas corresponds to an Eopaleozoic orogen which, consists of Ordovician metamorphic rocks and migmatites and contains a series of Cambrian to Middle-Ordovician intrusive rocks varying from tholeiitic gabbros to granites. These intrusive rocks are associated with subduction that culminated in the Upper Ordovician to Lower Devonian (Ramos, 1999). During the Lower Carboniferous, post-orogenic granites were emplaced. The internal structures of the crystalline basement are complex and consist of products of the different cycles of deformation, metamorphism and magmatic events (Ramos, 1999). The basement is partly covered with continental sedimentary rocks of Carboniferous, Permian and Tertiary age (Ramos, 1999).

2.1. Geology of the Sierra de Velasco

The Sierra de Velasco (Fig. 1) is located in the northwest of the La Rioja city and is composed of mainly granitoids with different crustal levels of emplacement, deformation, chemical composition and age of crystallization. The granitoids have contrasting age dates, which vary between Lower Ordovician and Lower Carboniferous. In the eastern part of the Sierras de Velasco, low-grade metamorphic rocks are exposed, which can be correlated with the La Cébila Formation (González Bonorino, 1951), and have recently been dated using marine fossils (Verdecchia et al., 2007) to be Lower Ordovician in age.

The Sierra de Velasco was affected by dynamic metamorphism that resulted in subvertical units, which formed a deformation zone. The western part of the Sierra de Velasco is composed of variably deformed granitoids, whereas the central and northern sectors consist of predominantly undeformed syenite, monzogranite and two-mica porphyry granite (Báez et al., 2005). In the south, granodiorites and tonalites with biotite, hornblende and titanite indicate a different genesis compared to granitoids in the other parts of the mountain chain (Bellos et al., 2002). In the extreme north and in the central sector of the Sierra de Velasco, the undeformed San Blas, El Durazno and Huaco granite stocks are exposed (Figs. 2 and 3). Sedimentary rocks are sparsely represented in the Sierra de Velasco. In the central and southern sector, sedimentary rocks appear to be arenites of the Upper Carboniferous Libertad Formation and the Permian Sauces and Prudencia Formations (Amos and Zardini, 1962). The Tertiary is exposed in the north in the Salicas Formation and alluvial sediments of Quaternary age.

2.2. Geology of the Sierra de Mazán

The Sierra de Mazán is a nearly north–south oriented mountain belt in the northeastern part of the La Rioja city (Figs. 1 and 4). The oldest rocks correspond to the La Cebila Formation (González Bonorino, 1951), which consist of quartz-muscovite phyllites striking predominantly northwest–southeast and dipping 50° to 55° northeast (or southwest), and outcropping mainly in the south

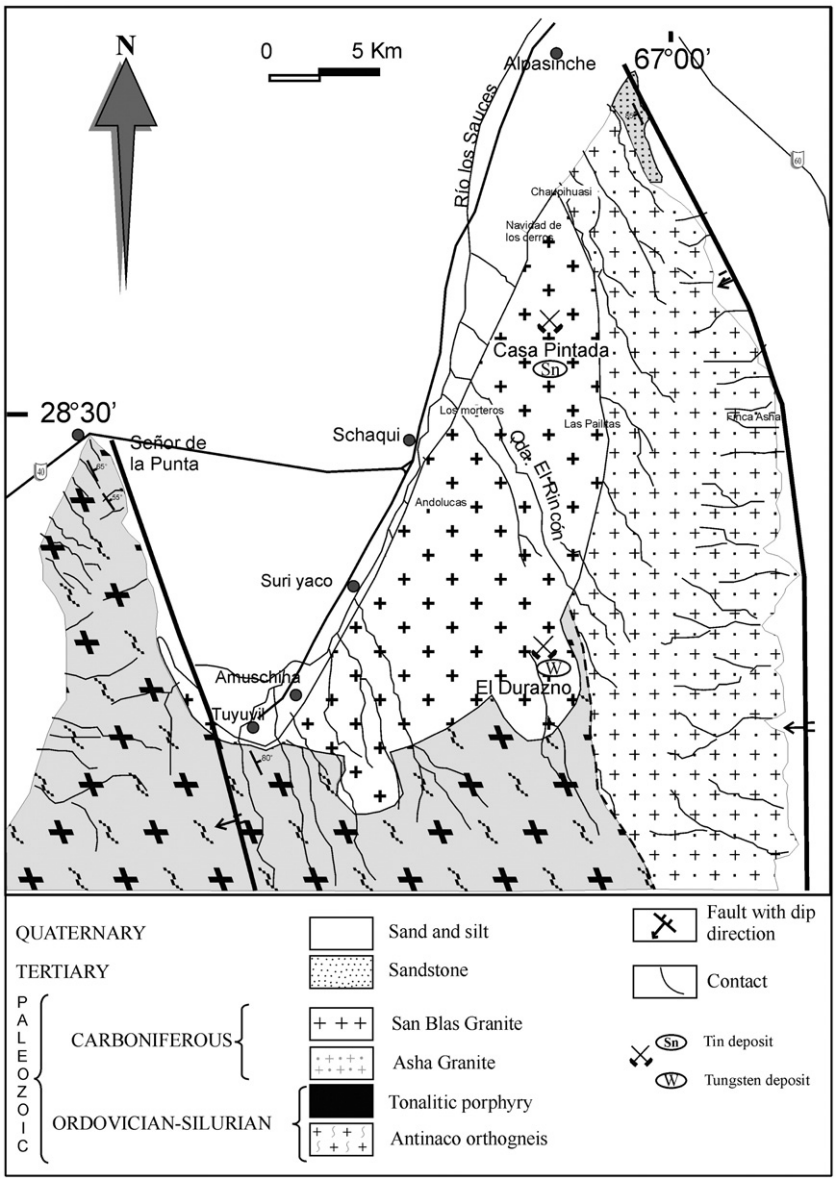

Fig. 2. Geological location map of the northern part of the Sierra de Velasco. Modified after Báez (2006).

and west of the mountains. These rocks were intruded by the Mazán granite (Fogliata and Ávila, 1997) of Ordovician–Silurian age (Stipanicic and Linares, 1975), which in the south is bordered by a mylonitic belt (Toselli and Toselli, 1990). The Mazán granite is a large porphyry hosting Sn–W deposits (Fig. 4). The inequigranular La Quebrada granite (Fogliata and Ávila, 1997) intruded the Mazán granite (Fig. 4). In addition, vein-shaped pegmatites and aplite, granite, and quartz–granite dikes are observed (Fogliata, 1999). The Cenozoic corresponds to arenites of the Tertiary Salicas Formation and sedimentary rocks of the Quaternary Coneta Formation. The latter are composed of Lower Holocene fluvial and Upper Holocene eolian sediments.

2.3. Geology of the Cerro Negro

This mountain chain is located in the southeast of the Catamarca province and composed of Paleozoic crystalline basement (Fig. 5). The northern part is characterized by deformed tonalites, whereas in the south an undeformed calc-alkaline granite stock is exposed. This stock is in contact with tonalites of the Cerro Colorado (Martínez, 1978). The overlying units consist of clastic continental sedimentary rocks of the Pliocene Sálicas Formation and the Pleistocene Las Cumbres Formation (Bossi et al., 1996). Modern sediments include alluvial fans and Eolian deposits.

2.4. Geology of the Sierra Ancasti

The Sierra Ancasti is located in the southeastern part of the Catamarca province (Fig. 1). It is elongated in a southern direction, is asymmetrical with gently dipping eastern and steeply dipping western parts. The oldest rocks are part of the Ancasti Formation, which correlate with the Early Ordovician La Cébila Formation. These Formations are composed of fine bands of mica schist and felsic calc-silicates. Tonalites and granodiorites are Late Carboniferous

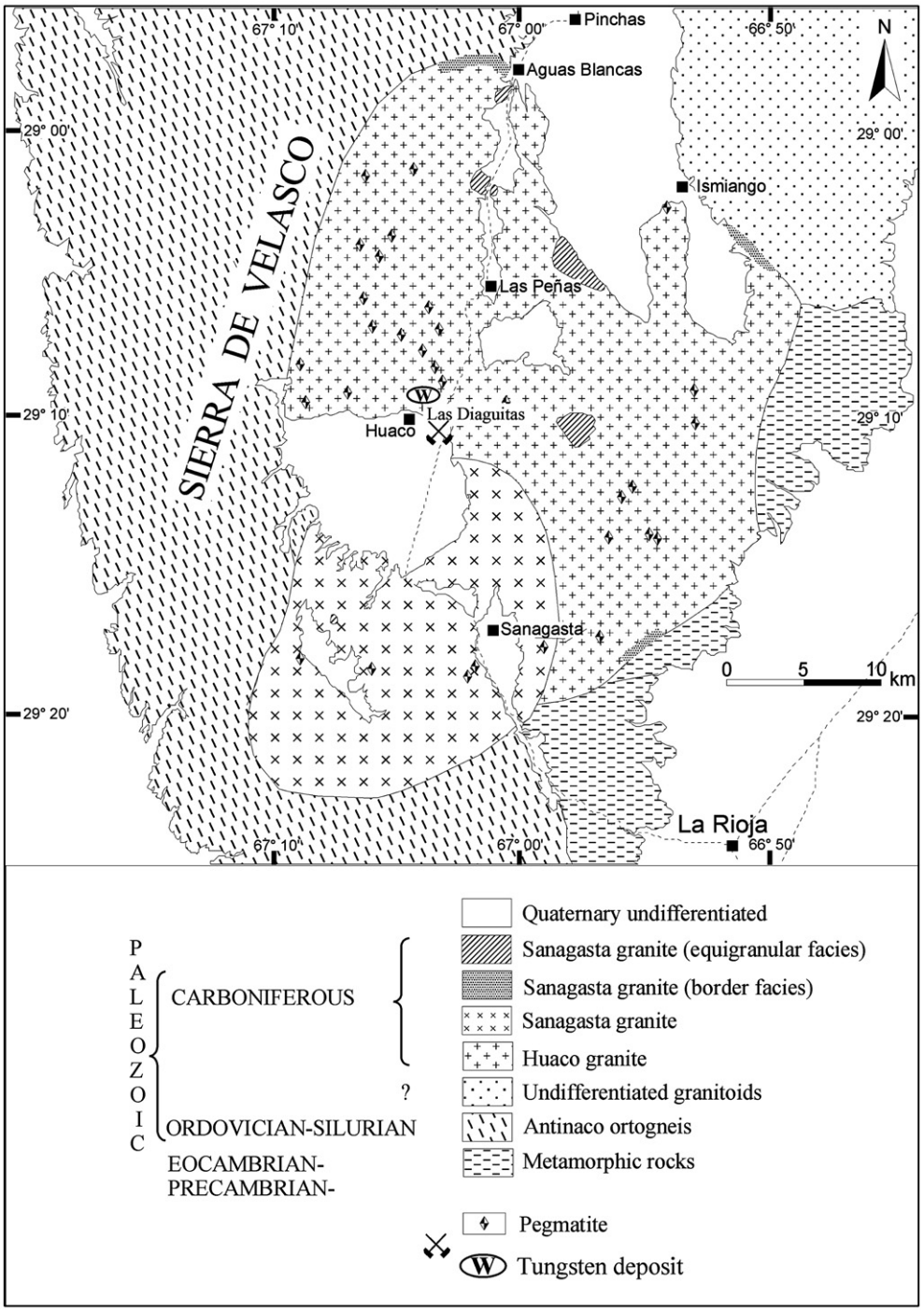

Fig. 3. Geological map of the central part of the Sierra de Velasco. Modified after Sardi (2005).

stocks intruding into the metamorphic country rocks (Fig. 6). Other juvenile late tectonic plutons consist of tonalities, biotite granodiorites and biotite-muscovite-garnet bearing granites, which appear to be emplaced as discordant bodies. The last expression of plutonic activity is the emplacement of pegmatites containing muscovite, spodumene, beryl and tourmaline. The Late Paleozoic is represented by acid volcanic rocks, Carboniferous tuff and basalts, and Permian continental arenites deposited unconformably over the crystalline basement. The oldest Quaternary sedimentary rocks consist of fanglomerates and arenites deposited unconformably at the foot of the mountain chain.

3. Granitoid-associated Sn–W mineralization in the Sierras Pampeanas

Significant Sn–W mineralization in the Sierras Pampeanas is associated with post-orogenic Carboniferous granitoids (Fig. 1). The most important Sn–W regions (Fig. 1) include those that are subjects of this investigation. The Sn–W mineralization in the Sierras de Mazán has been studied in detail by Fogliata (1999), Fogliata et al. (1998) and Fogliata and Ávila (2001) and, therefore, only a brief summary is provided here. The Sn–W mineralizations in the Sierras de Velasco,

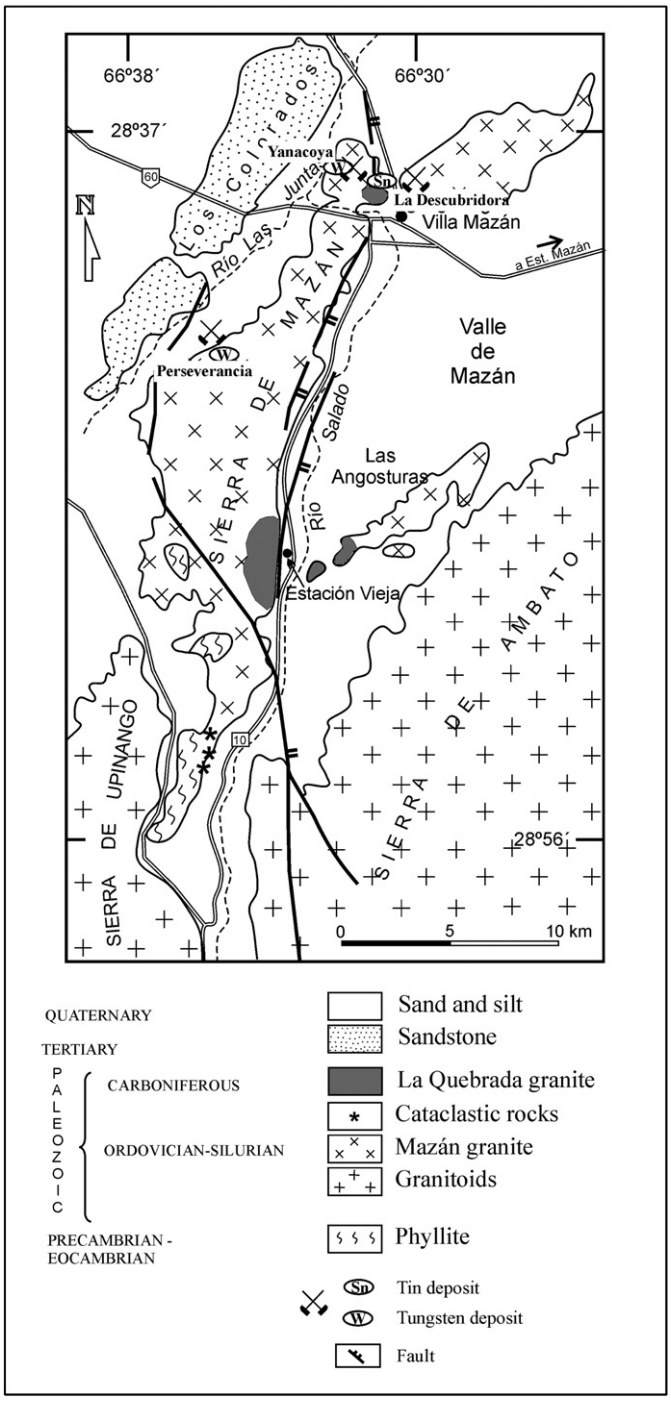

Fig. 4. Geological map of the Sierra de Mazán. Modified after Fogliata (1999).

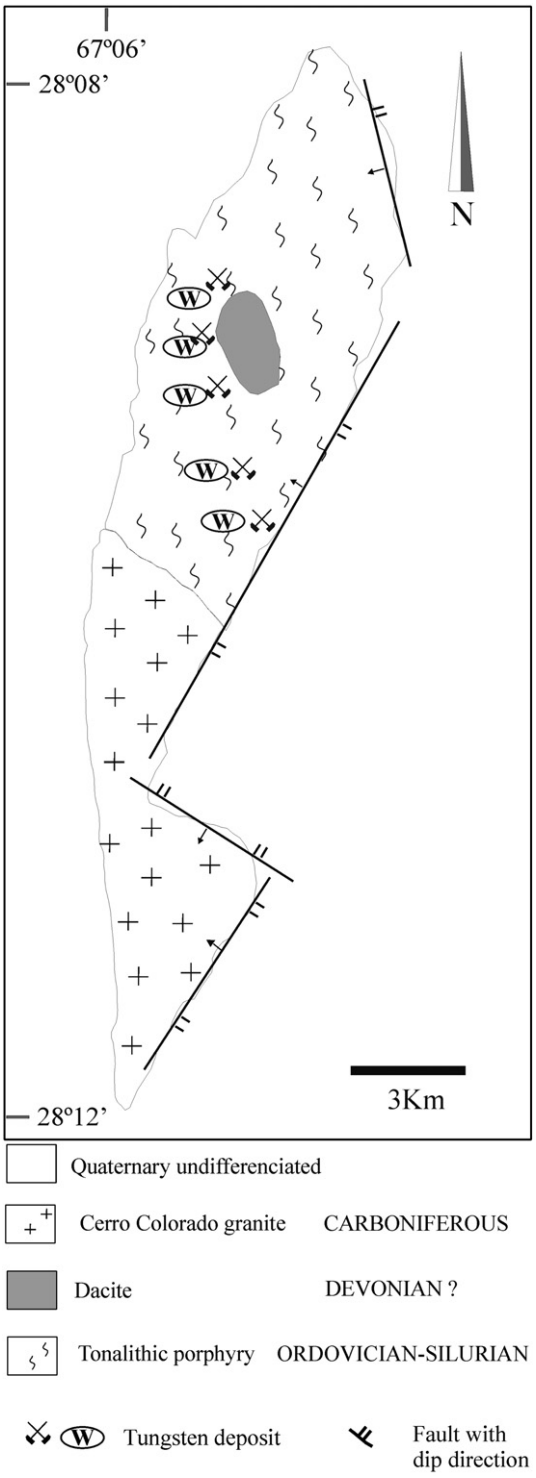

Fig. 5. Geological map of the Cerro Negro. Modified after Martínez (1978).

Ancasti and Cerro Negro are less known and only partial descriptions of the geology of abundant mines are available. Currently, there is only limited exploration for and exploitation of Sn and W in the Sierras Pampeanas.

3.1. The San Blas, Huaco and El Durazno granitoids in the Sierra de Velasco

The high-level, post-tectonic San Blas granite stock is exposed in the northern part of the Sierras de Velasco (Fig. 2) and dated 334 ± 5 Ma (conventional U–Pb on zircons; Báez et al., 2004) and 340 ± 3 Ma (U–Pb SHRIMP on zircons; Dahlquist et al., 2006). The central zone of the granite stock was investigated in an area called Casa Pintada (Fig. 2). The yellow syeno-monzogranite at Casa Pintada has a porphyritic texture and is composed of quartz, megacrystals of perthitic microcline, plagioclase, biotite, zircon, titanite and fluorite. It contains miaroles of 6 to 8 cm in diameter filled with quartz and tourmaline. An approximately 100 m wide corridor contains abundant aplitic veins (0.4 to 0.5 m in width), which are composed of

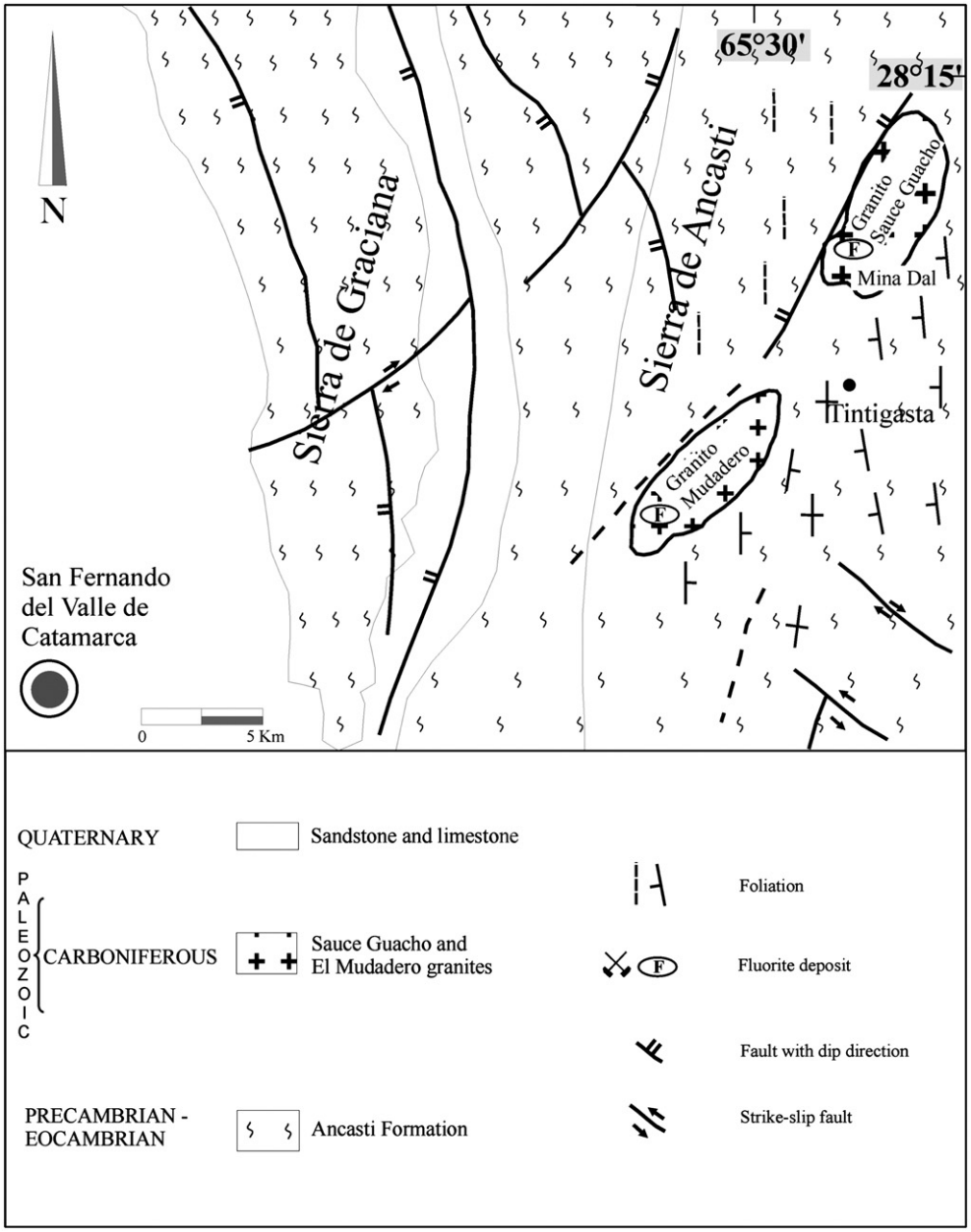

Fig. 6. Geological map of the Sierra de Ancasti.
Modified after Toselli et al. (1983).

quartz, plagioclase, potassic feldspar (microcline) and apatite. Selective and pervasive hydrothermal alteration in the central zone of the San Blas granite is characterized by chlorite–biotite–tourmaline. Chlorite replaced the igneous biotite. Multiple veinlets contain anhedral biotite and tourmaline which overprint the igneous minerals.

In the northern zone of the Sierra Velasco, where the San Blas granite is exposed, Cravero (1983) described an alluvial Sn deposit with detrital cassiterite in the Casa Pintada area and a quartz–muscovite–tourmaline vein with 6% Sn. In the same area, Cravero (1983) described a north–south striking and subvertical dipping, approximately 0.90 m wide quartz–tourmaline vein with disseminated hematite crystals and pockets of cassiterite with up to 250 ppm Sn.

The undeformed, subrounded El Durazno granite stock is located southeast of the San Blas granite (Fig. 2), has a surface area of 8 km^2 and intruded into deformed Ordovician Antinaco orthogneiss. It is a white syeno-monzogranite, displaying an equigranular texture and is composed of quartz, potassic feldspar, plagioclase, biotite, apatite and zircon. The granite has subcircular black clusters (up to 4 cm) of biotite and iron oxides. At the northern border of the El Durazno granite, wolframite was exploited in the 1940's from quartz veins hosted in the metamorphic orthogneiss. The roughly 0.25 m wide veins are located in an irregular corridor, strike approximately north–south and have a thickness of <0.25 m. The hydrothermal alteration is characterized by quartz veins containing thin lamellae of muscovite.

The undeformed, post-tectonic Huaco syeno- to monzogranite stock (Grosse and Sardi, 2005) is a semi-ellipsoid stock in the central sector of the Sierras de Velasco (Fig. 3). It is dated 350 ± 5 Ma and 358 ± 5 Ma (conventional U–Pb on monazites) and 354 ± 4 Ma (LA-ICP-MS U–Pb on zircons) by Grosse et al. (2009) and Söllner et al. (2007), respectively. The Huaco stock intruded into metamorphic rocks of the La Cebila Formation in the east and southeast and into

variably deformed Ordovician granitoids in the west. The Huaco granite has a porphyritic texture with megacrystals of perthitic microcline, up to 12 cm in length, and is composed of quartz, microcline, plagioclase, biotite, muscovite, apatite and zircon. It contains genetically related zoned pegmatites with pockets of beryl (Sardi, 2005). The closed underground Las Diaguitas W mine contains a lode that strikes north-northwest and is composed of quartz, wolframite (with 71.5% of WO_3), tourmaline, molybdenite, magnetite, pyrite, bismuth and traces of chalcopyrite (De Alba, 1979). Wolframite occurs as idiomorphic to subidiomorphic crystals. It is associated with quartz and idiomorphic garnets.

3.2. The La Quebrada granitoid in the Sierra de Mazán

The main outcrops of the post-tectonic, epizonal La Quebrada granite stock are located in the northern and south-eastern part of the Sierra de Mazán (Fig. 4). The pink to white-yellow, medium to fine grained granite stock has a monzogranitic composition and displays granular texture. It intruded the Mazán porphyritic granite. The La Quebrada granite is composed of quartz, microcline, plagioclase (albite), muscovite, apatite, zircon, tourmaline, monazite and locally andalusite, and opaque minerals such as pyrite and arsenopyrite (Fogliata, 1999). La Quebrada granite has pegmatite veins with large crystals of tourmaline in the entire zone of the Estación Vieja (Fig. 4). In the Sierra de Mazán, the granite-related mineralization consists of greisen type Sn–W deposits. Fogliata and Ávila (2001) define two types of greisens: quartz–muscovite–tourmaline and muscovite–quartz–topaz–tourmaline. These Sn–W deposits are vein-hosted, for example the La Descubridora (Sn) and Yanacoya (W) deposits. The Perseverancia (W) deposit contains veinlets within the greisens. The cassiterite and wolframite mineralization is disseminated and accompanied by scheelite, chalcopyrite, arsenopyrite, pyrite, sphalerite, ilemite–rutile, hematite, scorodite and gypsum (Fogliata and Ávila, 2001). The hydrothermal alteration related to the greisen is principally observed in the porphyritic Mazán granites, which host the Sn–W deposits, and occurs as bands at the contact with the La Quebrada granite and

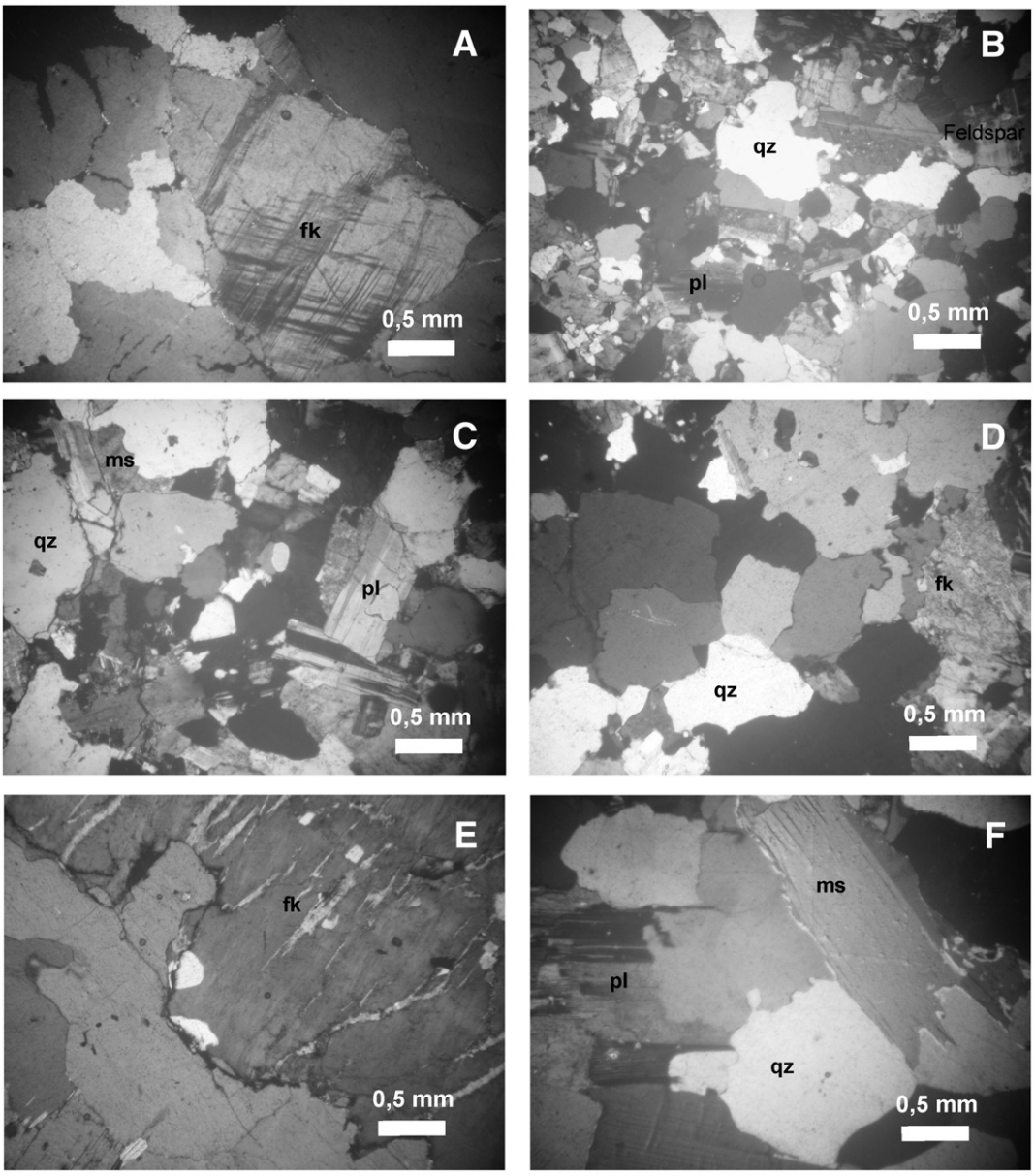

Fig. 7. Photomicrographs of selected samples of unaltered Carboniferous granites from the western Sierras Pampeanas which were used for petrographic and geochemical analyses.

the quartz veins. The intense and pervasive alteration completely masks the original texture of the Mazán granite.

3.3. The Cerro Colorado granitoid in the Cerro Negro

The Cerro Colorado granite is located in the south of the Cerro Negro, at the western side of the Rio Salado. Its northern limit is in contact with the basement, which it intrudes (Fig. 5). The pink colored rock is a porphyritic syenogranite (Martínez, 1978) containing microcline phenocrysts and a matrix of quartz, microcline, plagioclase (oligoclase), biotite, and in minor proportions muscovite, sericite, apatite, zircon and various disseminated opaque minerals. This granite also contains pegmatites and aplite dikes. Hydrothermal alteration consists of chlorite and sericite. The chlorite is locally replaced by sericite. Five abandoned W mines are located in the western part of the Cerro Negro. The main ore minerals – scheelite and wolframite – and traces of native gold, pyrite and chalcopyrite are disseminated in approximately NNE-striking quartz–tourmaline–feldspar veins.

3.4. The Sauce Guacho and Mudadero granitoids in the Sierras Ancasti

The oval Sauce Guacho granite stock (Fig. 6) is about 10 km long, approximately NE–SW shaped, and is exposed in the northeast of the Sierra de Ancasti (Fig. 6). The granite is tentatively dated at 334 ± 11 Ma (whole rock by Rb–Sr; Knüver, 1983) and intruded into metamorphic rocks of the Ancasti Formation (Toselli et al., 1983). The pink syeno- to monzogranite is medium to coarse grained, varies from inequigranular to porphyritic texture and contains quartz, microcline, plagioclase (oligoclase), muscovite, and minor quantities of biotite, garnet and opaque minerals. In the granite, pervasive hydrothermal alteration consists of sericite–chlorite–fluorite, which selectively replaced feldspars and micas, and veinlets of fluorite and quartz. The Sauce Guacho granite is exposed at the abandoned Dal mine, which is characterized by a hydrothermal fluorite and quartz vein.

The Mudadero granite is exposed southeast from the Sauce Guacho granite (Fig. 6) and is tentatively dated at 373 ± 10 Ma (biotites by Rb–Sr; Knüver, 1983). The suboval syenogranite stock strikes NW–SE (Toselli et al., 1983). The reddish granite displays locally a porphyritic texture with two distinct aplitic and granular facies

Table 1
Whole rock major oxide analyses (in wt.%) of selected samples from granite stocks in the Sierras Pampenas orogen, northwestern Argentina.

Sample	SiO_2	AL_2O_3	Fe_2O_3	FeO	MgO	CaO	Na_2O	K_2O	TiO_2	MnO	P_2O_5	LOI	Total
Detect. Limit	0.50	0.03	0.10	0.10	0.02	0.01	0.04	0.005	0.004	0.004	0.002		
El Durazno granite stock (Sierra de Velasco)													
ED5	75.88	13.92	0.76	0.48	0.05	0.33	3.54	4.45	0.05	0.13	0.27	0.63	100.50
ED6	73.49	15.45	0.82	0.52	0.02	0.50	5.47	2.51	0.03	0.16	0.35	0.44	99.75
ED7	74.16	14.79	0.66	0.25	0.01	0.32	4.75	3.73	0.02	0.23	0.26	0.49	99.67
ED9	73.95	15.19	0.76	0.57	0.01	0.42	4.30	4.09	0.03	0.08	0.33	0.40	100.12
ED10	74.58	14.85	0.59	0.29	0.01	0.43	4.46	3.86	0.02	0.11	0.31	0.52	100.03
La Quebrada granite stock (Sierra de Mazán)													
SM13	75.76	14.67	1.00		0.07	0.40	5.48	2.30	0.05	0.06	0.37	0.42	100.56
SM15	75.33	14.48	0.79	0.40	0.05	0.34	4.40	3.76	0.05	0.04	0.29	0.52	100.45
SM103	74.37	14.71	1.45	na	0.01	0.33	4.36	3.87	0.06	0.04	0.26	0.50	99.96
Mazán barren granite stock (Sierra de Mazán)													
M18	68.66	15.73	4.78	na	1.78	0.97	2.23	4.26	0.68	0.09	0.19	1.48	100.86
Cerro Colorado granite stock (Cerro Negro)													
CN19	72.42	14.59	2.37	1.56	0.59	1.22	2.95	5.28	0.42	0.06	0.31	0.89	102.67
Mudadero granite stock (Sierra de Ancasti)													
23	75.58	13.71	0.78	0.37	0.14	0.44	3.10	5.50	0.09	0.05	0.28	0.65	100.69
26	75.45	14.51	0.85	0.40	0.19	0.41	3.64	4.34	0.10	0.07	0.28	0.96	101.20
27	75.18	14.35	0.95	0.12	0.18	0.51	3.32	4.54	0.11	0.07	0.37	0.99	100.70
Mudadero granite, granular facies (Sierra de Ancasti)													
24	71.56	14.65	2.38	1.42	0.67	1.16	3.03	5.03	0.46	0.09	0.38	0.76	101.59
25	73.28	14.32	2.07	0.92	0.53	0.91	3.27	4.67	0.38	0.06	0.29	0.83	101.52
Sauce Guacho granite stock (Sierra de Ancasti)													
1	76.19	13.40	0.86	0.21	0.15	0.32	3.15	5.17	0.15	0.02	0.19	0.58	100.39
31	75.96	13.68	0.84	0.28	0.17	0.30	3.03	5.34	0.12	0.03	0.21	0.68	100.63
32	75.04	14.15	1.00	0.33	0.18	0.47	3.22	5.29	0.14	0.03	0.24	0.77	100.85
San Blas granite stock (Sierra de Velasco)													
SB104	74.50	11.80	2.75	na	0.04	0.80	2.99	5.24	0.13	0.04	0.02	1.70	100.01
SB105	76.66	13.28	1.70	na	0.22	0.69	5.03	1.72	0.28	0.02	0.25	0.10	99.95
San Blas barren granite (porphyritic facies) stock (Sierra de Velasco)													
SBP 6521	68.44	15.20	4.03	na	1.52	2.78	2.74	3.68	0.51	0.08	0.19	1.27	100.44
Huaco granite stock (Sierra de Velasco)													
H6587	73.94	13.22	2.57	na	0.24	0.88	2.88	5.32	0.23	0.07	0.15	0.98	100.48
H6590	73.99	12.81	2.28	na	0.30	0.91	2.79	4.91	0.22	0.04	0.22	0.96	99.43

Abbreviations: bdl = below detection limit; na = not analyzed.

documented. Igneous minerals in the granite include quartz, perthitic microcline, plagioclase, biotite, muscovite, zircon, apatite and euhedral opaques. The hydrothermal alteration minerals are kaolinite–sericite and sericite–chlorite, which replaced the igneous micas and feldspars. The Mudaderos granite is associated with various fluorite mines displaying similar characteristics as the Dal mine.

4. Granitoid geochemistry

4.1. Sample selection

A total of 23 granite samples were collected from outcrops in the western Sierras Pampeanas and were geochemically analyzed. The granite samples are from the Sierra de Velasco (San Blas, El Durazno and Huaco granite stocks), Sierra de Mazan (La Quebrada granite stock), Cerro Negro (Cerro Colorado stock) and Sierra de Ancasti (Mudadero and Sauce Guacho stocks). For petrography and geochemical analyses, care was taken to select granite samples that were devoid of hydrothermal alteration and deformation (Fig. 7).

4.2. Geochemical analyses

The samples were crushed with a steel jaw crusher at the University of Tucumán to a size of 1 to 2 cm. Crushed rock samples were milled and analyzed for major and trace elements at the Department of Earth Sciences Royal Holloway (DESRH) University of London (England) and for REEs at the Acme laboratory at Vancouver (Canada). Major oxides and trace elements were analyzed with X-ray fluorescence (XRF) spectrometry in wt.% and ppm, respectively. Major oxides were analyzed on fusion beads using flux with La_2O_3 heavy absorber and calculated on a volatile free basis. Trace elements were analyzed on pressed pellets and calculated on a 'wet' basis. The accuracy of major oxides analysis for the international granite standard MAN lies within typical uncertainty of the XRF data except P_2O_5 (see Thirlwall et al., 1997 for information on this standard). The precision (two standard deviations (2σ)) of major oxide analysis of six laboratory replicates was within 0.10 wt.%. The accuracy of trace element analysis for the international standard NIM-G lies within typical uncertainty of the ICP-MS data (see Thirlwall et al., 1997 for information on this standard). The precision (2σ) of trace element analysis of six laboratory replicates was within 3 ppm, except Ba

Table 2
Trace element analyses (in ppm) of selected samples from granite stocks in the Sierras Pampeanas orogen, northwestern Argentina.

Sample	Ba	Cr	Cs	Ga	Ge	Li	Nb	Pb	Rb	Sn	Sr	Th	Tl	U	V	Y	Zn	Zr	Au	W
	ppm	ppm	ppm	ppm	ppm	ppm	ppm	ppm	ppm	ppm	ppm	ppm	ppm	ppm	ppm	ppm	ppm	ppm	ppb	ppm
Detection limit	2	1	4	2	1	0.5	0.6	0.8	0.8	3	2	1.5	0.8	1	3	0.6	0.8	1.5	1	0.5
El Durazno granite stock (Sierra de Velasco)																				
ED5	30	3	19	23	3	124	35	13	636	9	9	5	3	2	6	7	38	17	5	42.4
ED6	28	12	bdl	20	7	277	51	13	468	5	77	8	3	3	6	4	91	16	29	6.6
ED7	29	7	4	22	5	483	41	10	782	4	49	5	4	5	15	6	56	18	10	4.7
ED9	16	8	21	22	6	421	27	10	831	5	31	5	5	3	6	7	39	12	3	2.8
ED10	10	3	6	26	4	240	29	12	790	3.2	23	2	4	6	6	5	60	14	1	5.4
La Quebrada granite stock (Sierra de Mazán)																				
SM13	7	2	196	22	5	na	19	5	521	49	12	bdl	2	2	12	9	59	14	na	7.7
SM15	9	35	58	23	4	137	21	7	524	40	12	bdl	3	1.4	7	7	45	19	8	10.0
SM103	3	na	52	23	na	na	20	na	511	41	16	2	bdl	2	bdl	4	na	14	na	10.9
Mazán barren granite (Sierra de Mazán)																				
SM18	455	58	16	20	2	48	16	21	193	7	95	12	bdl	3	77	27	69	164	bdl	bdl
Cerro Colorado granite stock (Cerro Negro)																				
CN19	288	8	25	22	2	131	23	29	334	9	72	24	2	5	32	24	64	163	bdl	4.3
Mudadero granite stock (Sierra de Ancasti)																				
23	65	22	25	23	2	117	29	26	499	5	30	4	3	2	12	13	20	30	4	13.5
26	15	3	16	27	2	99	38	14	627	5	15	4	4	3	13	12	184	37	bdl	31.5
27	41	27	17	27	2	102	41	12	642	8	25	5	3	2	15	14	282	37	6	17.0
Mudadero granite, granular facies (Sierra de Ancasti)																				
24	327	27	45	23	2	181	25	28	437	7	100	39	3	4	43	21	86	194	2	4.0
25	235	38	33	23	2	149	24	25	399	7	91	27	2	3	38	21	71	154	bdl	11.9
Sauce Guacho granite stock (Sierra de Ancasti)																				
1	136	2	14	19	2	85	18	25	437	bdl	46	7	2	1.2	13	9	24	46	bdl	6.8
31	75	27	16	21	2	114	26	21	475	6	34	6	3	1.1	10	10	37	39	bdl	15.8
32	96	29	12	22	2	89	25	24	444	5	42	6	2	2	20	12	28	47	4	25.6
San Blas granite (Sierra de Velasco)																				
SB104	53	na	bdl	27	na	na	75	na	548	13	16	58	1.0	11	bdl	105	na	218	na	6.5
SB105	39	na	19	19	na	na	31	na	261	177	20	37	bdl	4	9	24	na	212	na	9.6
San Blas barren granite (Sierra de Velasco)																				
SBP6521	241	35	7	16	na	na	15	20	174	4	91	11	1.2	2	67	26	55	134	na	5.8
Huaco granite stock (Sierra de Velasco)																				
H6587	185	na	37	24	na	na	45	na	457	19	46	45	3	16	8	65	na	221	na	6.4
H6590	181	na	21	20	na	na	30	na	343	12	48	29	3	10	11	38	na	181	na	3.4

Abbreviations: bdl = below detection limit; na = not analyzed.

(6 ppm), Cr (13 ppm) and Ni (3.7 ppm). The samples for REE analyses were fused in graphite crucible at 950 °C before they were analyzed in an inductively coupled plasma mass spectrometry (ICP-MS) using a Perkin Elmer Elan 5000 instrument. The accuracy of REE analysis for the international standard NIM-G lies within typical uncertainty of the ICP-MS data. The precision (2σ) of REE analysis of a laboratory replicate was within 15%, except Eu (32%), Gd (25%), Yb (16%) and Lu (43%). Detection limits for major oxide, trace elements and REEs are provided in Tables 1, 2 and 3, respectively.

The major oxide FeO was determined (in wt.%) using the volumetric titration method at Ultra Trace Pty. Ltd. in Perth. Precision of a repeat sample was within 14% relative error. Gold, Pt, Pg (in ppb) and Li (in ppm) were also analyzed at Ultra Trace Pty. Ltd. Gold, Pt and Pd were analyzed by firing and cupellation of a 40 g portion of a sample following the fire assay process. The noble metal prills we parted with nitric acid, dissolved in aqua regia and diluted for ICP-OES analyses. Precision of a repeat sample was 20% relative error. Lithium was determined by ICP-MS with a sub-sample digested with sulphuric and hydrofluoric acids. Precision of a repeat sample was 5% relative error.

4.3. Results

The whole rock major element, trace element and REE data of the various granitoid samples are presented in Tables 1, 2 and 3, and compared to the average geochemical composition of granite as defined by Krauskopf (1979) in Kamilli and Criss (1996).

4.3.1. Major oxide

All of the analyzed granitoids are rich in SiO_2 (>72%), present normal K, and, with respect to CaO values (Table 1), are similar in content to the normal granites of Tischendorf (1977). The highest Na_2O values with respect to the content of normal granites (cf. Tischendorf, 1977) are best represented by the El Durazno, San Blas (aplitic facies) and La Quebrada granite stocks (Table 1). The majority of the studied granitoids are peraluminous with Aluminium Saturation Index (ASI) between 1.05 and 1.38 (Fig. 8). In addition, all granites are evolved (high Rb/Sr ~1 to 100) and display an intermediate oxidation state (Fe_2O_3/FeO ~0.1 to 1.0). In the SiO_2 versus $Na_2O + K_2O$ diagram, all the studied granitoids fall within the Sn–W field (Baker et al., 2005; Fig. 9). It is important to note that this result pertains also to the granitoids of the Sierra Ancasti, even though no Sn–W mineralization has been reported yet from at area.

4.3.2. Trace elements

In the modified ternary Rb–Ba–Sr diagram of El Bousely and El Sokkary (1975), it is clear that all of the studied granites are highly fractionated, with the La Quebrada and El Durazno granite stocks being the most fractionated, the Mudadero, San Blas, Sauce Guacho

Table 3
REE analyses (in ppm) of selected samples from granite stocks in the Sierras Pampeanas orogen, northwestern Argentina.

Sample	La	Ce	Pr	Nd	Sm	Eu	Gd	Tb	Dy	Ho	Er	Tm	Yb	Lu	Suma REE	La_N/Lu_N	Eu/Eu *
Detection limit	0.1	0.1	0.02	0.3	0.05	0.02	0.05	0.01	0.05	0.02	0.03	0.01	0.05	0.01			
El Durazno granite stock (sierra de Velasco)																	
ED5	2.800	5.500	0.720	2.700	0.580	0.060	0.460	0.100	0.680	0.130	0.460	0.100	0.890	0.150	15.33	2.00	0.35
ED6	1.200	1.900	0.260	0.800	0.160	0.040	0.150	0.050	0.160	0.060	0.140	0.050	0.280	0.080	5.33	1.60	0.79
ED7	1.800	2.600	0.440	1.700	0.340	0.080	0.320	0.080	0.310	0.090	0.210	0.070	0.390	0.090	8.52	2.14	0.74
ED9	1.700	3.300	0.400	1.400	0.360	0.030	0.280	0.060	0.350	0.090	0.250	0.060	0.490	0.080	8.85	2.30	0.29
ED10	1.500	1.600	0.260	0.900	0.190	0.030	0.190	0.040	0.220	0.060	0.170	0.040	0.310	0.060	5.57	2.70	0.48
La Quebrada granite stock (sierra de Mazán)																	
SM13	1.400	3.400	0.420	1.500	0.510	bdl	0.370	0.090	0.400	0.080	0.200	0.050	0.490	0.090	9.0	1.7	0.07
SM15	39.500	90.900	11.360	45.300	7.370	0.840	5.360	0.750	3.660	0.700	1.910	0.310	1.990	0.330	210.3	12.8	0.41
SM103	1.900	4.200	0.590	2.100	0.700	0.020	0.550	0.120	0.720	0.100	0.360	0.070	0.670	0.100	12.2	2.0	0.10
Mazán barren granite (sierra de Mazán)																	
M18	43.176	90.009	10.513	43.207	8.988	1.551	8.593	1.519	7.705	1.464	3.931	0.569	5.296	0.605	227.1	7.7	0.55
Cerro Colorado granite stock (cerro Negro)																	
CN19	49.800	118.900	13.950	56.400	10.770	0.990	8.600	1.230	6.490	1.140	3.040	0.390	2.760	0.390	274.9	13.70	0.31
Mudadero granite stock (sierra de Ancasti)																	
23	6.800	13.200	2.040	8.400	1.860	0.270	1.520	0.280	1.690	0.350	1.080	0.180	1.250	0.180	39.1	4.0	0.49
26	10.400	17.400	2.620	10.200	1.910	0.170	1.520	0.260	1.490	0.260	0.760	0.110	0.910	0.120	48.1	9.3	0.30
27	10.700	20.500	2.990	12.400	2.380	0.250	2.000	0.320	1.880	0.340	0.990	0.140	1.060	0.150	56.1	7.6	0.35
Mudadero granite, granular facies (sierra de Ancasti)																	
24	53.900	130.400	15.340	60.700	10.070	0.950	6.730	0.850	3.950	0.670	1.910	0.260	1.970	0.270	288.0	21.4	0.35
25	2.400	6.600	0.850	3.200	0.950	<0.02	0.700	0.150	0.900	0.130	0.410	0.080	0.760	0.120	17.3	2.1	0.04
Sauce Guacho granite stock (sierra de Ancasti)																	
1	10.200	22.000	2.650	9.900	1.710	0.310	1.260	0.210	1.080	0.210	0.600	0.110	0.730	0.130	51.1	8.4	0.64
31	8.200	18.400	2.220	8.100	1.780	0.210	1.470	0.250	1.560	0.320	0.990	0.150	1.180	0.170	45.0	5.2	0.39
32	9.300	21.500	2.590	9.300	1.930	0.250	1.580	0.270	1.610	0.320	0.960	0.160	1.190	0.160	51.1	6.2	0.44
San Blas granite (sierra de Velaco)																	
SB104	89.400	185.300	23.610	83.600	16.730	0.400	14.770	2.930	18.260	3.450	10.400	1.570	9.600	1.220	461.2	7.9	0.08
SB105	13.900	31.600	4.170	15.700	3.940	0.220	3.860	0.820	5.010	0.830	2.420	0.410	2.510	0.330	85.7	4.5	0.17
San Blas barren granite (sierra de Velaco)																	
SBP 6521	23.000	48.600	5.790	21.400	4.830	0.900	4.060	0.810	4.610	0.900	2.500	0.410	2.430	0.350	120.6	6.7	0.62
Huaco granite stock (sierra de Velasco)																	
H6587	47.400	107.000	12.800	45.800	10.900	0.820	9.540	1.950	12.000	2.250	5.990	0.970	5.580	0.740	263.7	6.9	0.25
H6590	30.020	86.000	8.270	29.600	16.980	0.730	6.230	1.280	7.360	1.230	2.960	0.440	2.570	0.330	194.0	9.7	0.34

$Eu/Eu^* = Eu_N/(Sm_N.Gd_N)^{0.5}$

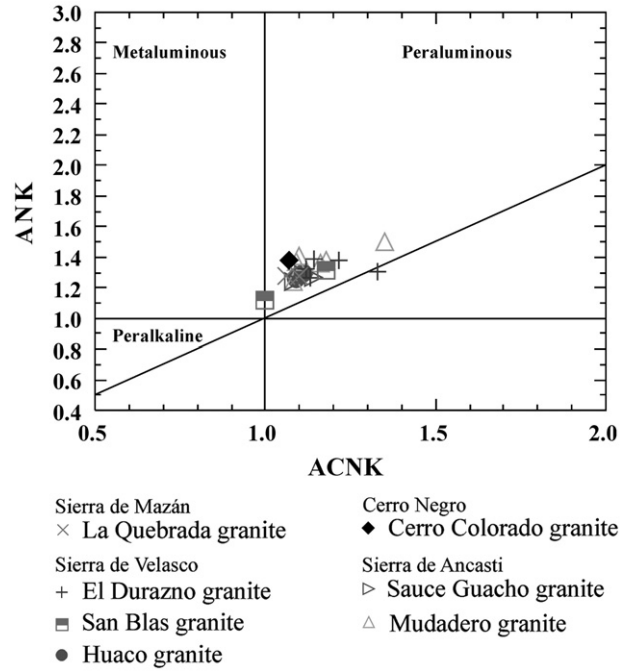

Fig. 8. Plots of the Sierras Pampeanas granitoids samples in the ANK versus ACNK diagram of Maniar and Piccoli (1989). ANK = $Al_2O_3/Na_2O + K_2O$ ACNK = $Al_2O_3/CaO + Na_2O + K_2O$ (molecular proportions).

and Huaco granite stocks being medium fractionated, and the Cerro Colorado granite stock being the least fractionated (Fig. 10). In the Ba versus Rb diagram (Fig. 11a), which is used to distinguish between mineralized (fertile) and barren granites (Dall Agnol et al., 1994; Ruiz et al., 2008; Tauson and Kozlov, 1973), the majority of samples fall in the fertile field, with respect to Sn–W mineralization, except samples from the Cerro Colorado, granular facies of the Mudadero granite stocks, and the Huaco granite (Fig. 11a). In the Sr versus Rb diagram, most of the granitoids plot in the fertile field with the exception of the Cerro Colorado, Mudadero granular facies and sample ED10C of the Durazno granite stock (Fig. 11b).

The concentrations of trace elements in the analyzed granitoids were normalized to worldwide average trace element abundance

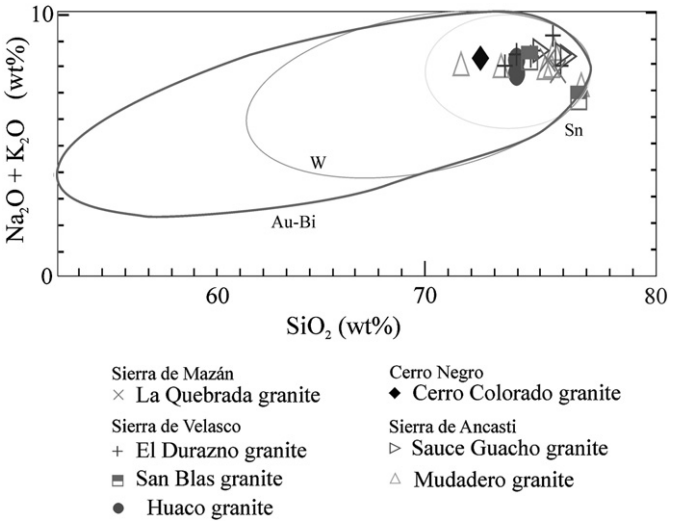

Fig. 9. Plots of the Sierras Pampeanas granitoid samples in the $Na_2O + K_2O$ versus SiO_2 diagram of Le Maitre (1989) and fields for typical Sn, W and Au–Bi bearing granitoids (Baker et al., 2005).

in granites (Fig. 12) in order to differentiate mineralized from barren granites as far as Sn–W mineralization is concerned. The mineralized granites display a strong difference with respect to unmineralized granites from the same area. The Mazán and San Blas barren granites have high Ba and low Rb contents. The granitoids associated with Sn–W mineralization are enriched in Rb, Sn and W (e.g., the La Quebrada and aplitic facies of San Blas granites), and display low Sr values (Fig. 12). The average content of Sn and W in unmineralized granites is approximately 6 ppm (Table 2). Mineralized granites, in contrast, contain an average of 64 ppm Sn in the La Quebrada and San Blas granites, 12 ppm W in the El Durazno granite and 9.6 ppm W in the La Quebrada granite (Table 2).

Using trace element discriminators, Srivastava and Sinha (1997) proposed the Geochemical Characterization Index (GCI)

$$GCI = \log_{10} \frac{Rb^3 \times Li \times 10^4}{Mg \times K \times Ba \times Sr}$$

for the differentiation of W-bearing and barren granites in India. The samples of mineralized granite with detectable Li plot in the GCI field of W granites (Fig. 13), whereas a sample of barren granites has a negative GCI. This indicates that the GCI can be used as an exploration tool. Positive GCI values were obtained from the Sierra de Ancasti granite, indicating its potential to host W mineralization.

4.3.3. REEs

The distribution of REEs can be used as a tool for discriminating between barren and mineralized granites (Irber, 1999; Monecke et al., 2002; Takahashi, et al., 2002). The analyses of lanthanides in the studied granitoids show major enrichment in light REEs, with respect to heavy REEs, and a negative Eu anomaly (Fig. 14). With respect to total REE concentrations the granite stocks can be subdivided in two groups. The first group comprises: the Huaco, Cerro Colorado, the

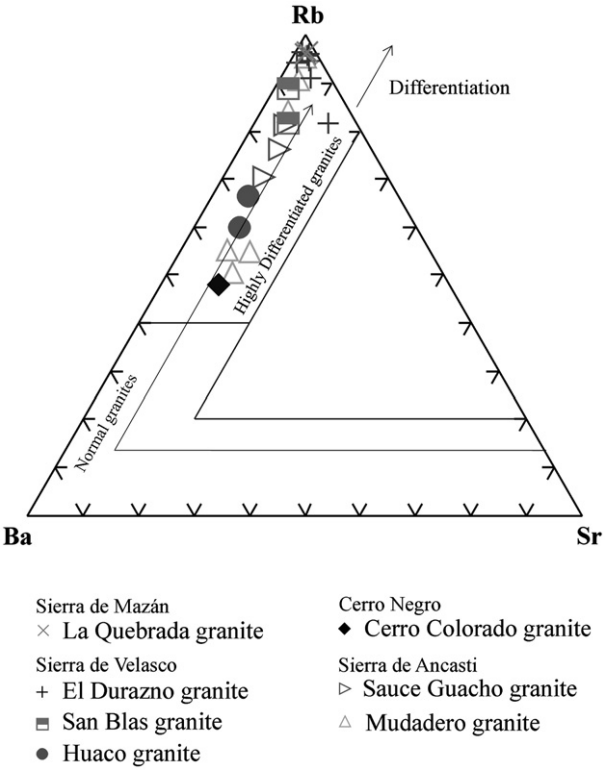

Fig. 10. Plots of the Sierras Pampeanas granitoid samples in the ternary Rb–Ba–Sr diagram. Modified from El Bousely and El Sokkary (1975).

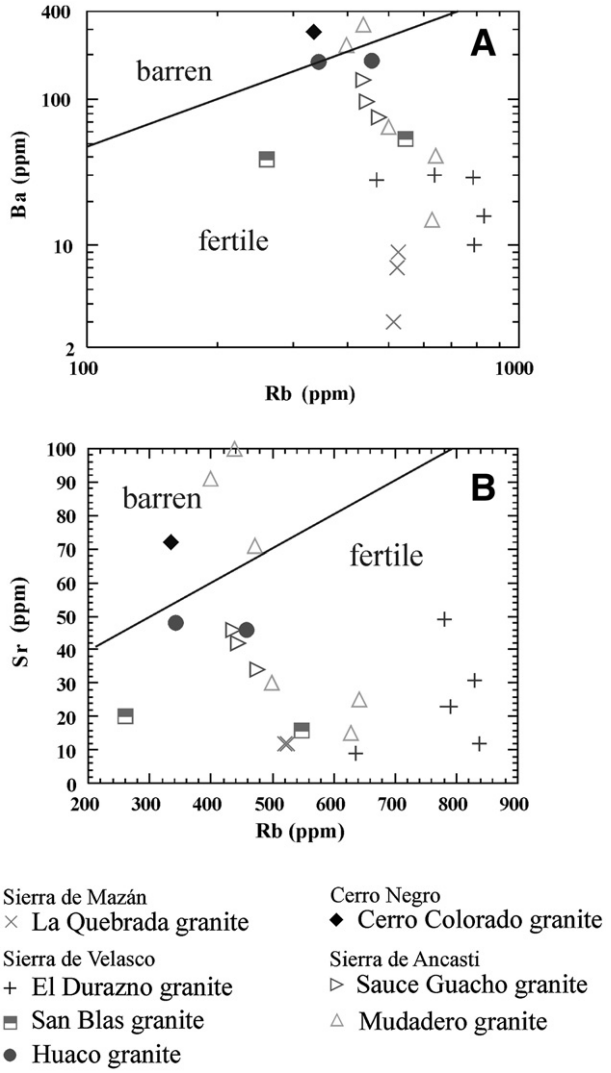

Fig. 11. Plots of the Sierras Pampeanas granitoid samples in diagrams of Ba versus Rb (a) and Sr versus Rb (b). With fields of barren and fertile granites from Olade (1980).

granular facies of the San Blas and Mudadero granite stocks, which have a total REE of >100 ppm. The second group of granitoids comprises the aplite facies of the San Blas, El Durazno, La Quebrada and Sauce Guacho stocks, which have a total REE of <100 ppm (Table 3). The La_N/Lu_N ratio normalized to chondrite C1 (Anders and Grevesse, 1989) is approximately 1 in the El Durazno and La Quebrada granite stocks and between 4 and 20 in the others granites (Table 3).

5. Geochronology

Three samples were selected for geochronology: sample CN19 from the Cerro Colorado granite stock in the Cerro Negro (Fig. 1), sample LD 1 from the granite stock in the Sierra de Mazán (Fig. 1) and sample SM 13 from the La Quebrada granite stock in the Sierra de Mazán (Fig. 1).

5.1. U–Pb SHRIMP analysis

The rock samples were crushed, milled and sieved through 60 mesh and the heavy minerals were separated using heavy liquid (TBE tetra-bromo-ethane; d = 3) and magnetic separation techniques. The final separation of the zircon was by hand picking the

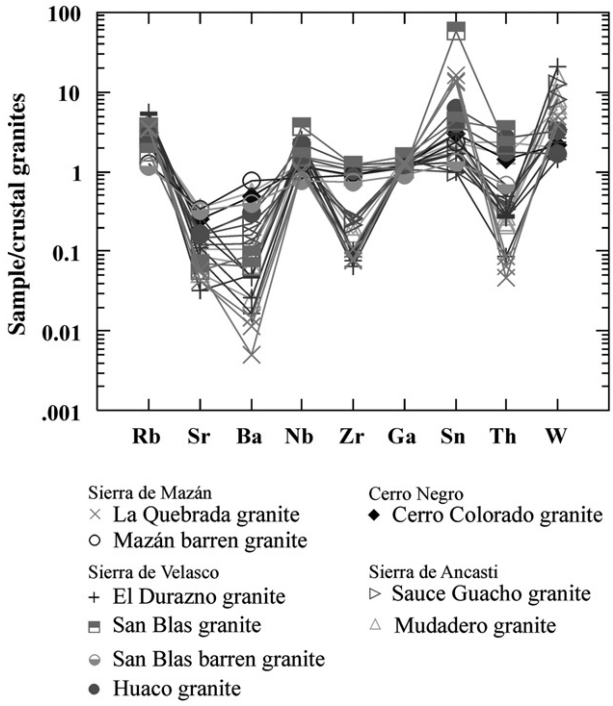

Fig. 12. Spider diagram of trace element contents of samples from the Sierras Pampeanas normalized to worldwide average crustal abundance of trace elements in granites from Levinson (1974).

grains. The zircons were mounted on epoxy disks with fragments of standards, ground and polished until nearly one third of each grain was removed, photographed in transmitted and reflected light, and imaged (backscattered electrons) for their internal morphology using a scanning electron microscope at the Centre for Microscopy and Microanalysis at the University of Western Australia. The epoxy mounts were then cleaned and gold-coated to have a uniform electrical conductivity during the SHRIMP analyses (Table 4).

The zircon standards used were BR266 (559 Ma, 903 ppm U) as the main standard and OGC1 (3647 Ma) to monitor the $^{207}Pb/^{206}Pb$ ratio. The isotopic composition of zircon was determined using SHRIMP II — Sensitive High-mass Resolution Ion MicroProbe (De Laeter and Kennedy, 1998), using methods based on those of Compston et al. (1992). A primary ion beam of ~2.5–4 nA, 10 kVO_2^{2-} with a diameter of ~25 μm was focused onto the mineral. Each zircon U–Pb analysis on SHRIMP used five to six scans collecting nine measurements on each ($^{196}Zr_2O$, ^{204}Pb, background, ^{206}Pb, ^{207}Pb, ^{208}Pb, ^{238}U, ^{248}ThO and ^{254}UO). Corrections for common Pb

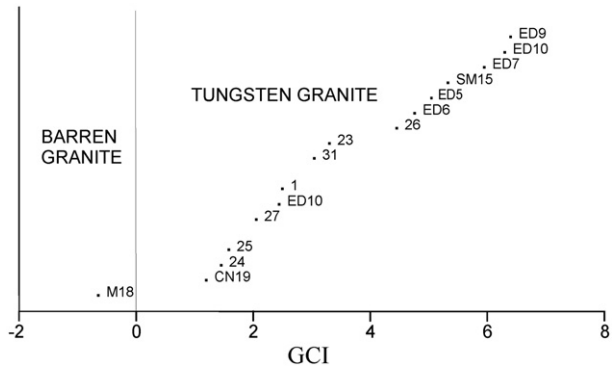

Fig. 13. Plots of the Sierras Pampeanas granitoid samples in a diagram of geochemical characterization index (GCI) and fields of W-bearing and W-barren granites from Srivastava and Sinha (1997).

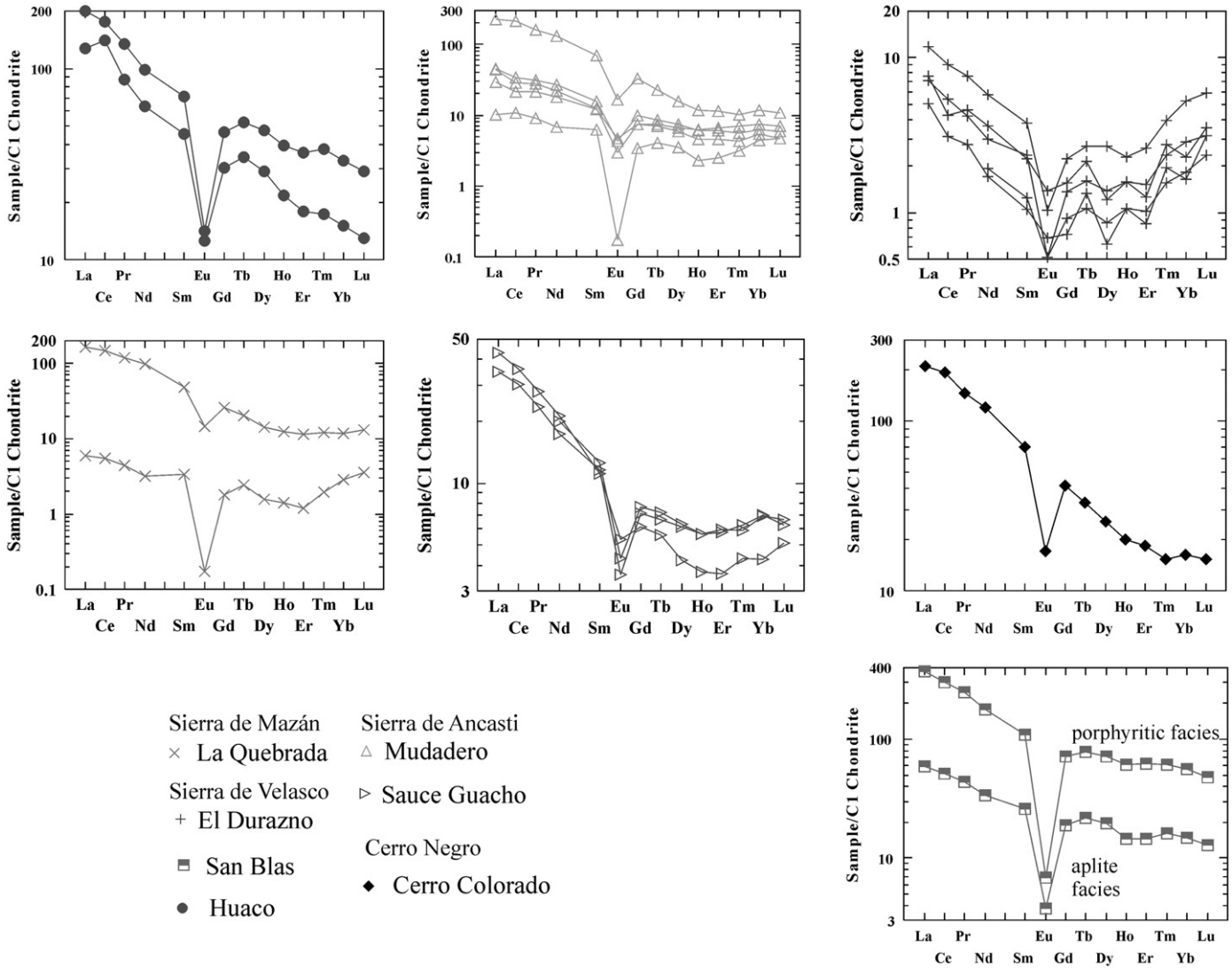

Fig. 14. REE concentrations in the studied samples of Sierras Pampeanas granites normalized to C1 chondrite (Anders and Grevesse, 1989).

were made using the measured ^{204}Pb and the Pb isotopic composition of Broken Hill galena. For each spot analysis, initial 60–90 s were used for pre-sputtering to remove the gold, avoiding the analysis of common Pb from the coatings. Zircons data are reduced using SQUID (Ludwig, 2002) software. Data were plotted on concordia diagrams using ISOPLOT/Ex software (Ludwig, 1999), in which error ellipses on concordia plots are shown at the 95% confidence level (2σ). All ages obtained are weighted mean $^{206}Pb/^{238}U$ ages.

5.2. Results

Sample CN19 (Cerro Colorado granite) has large and clear zircon crystals of 100–300 μm in length. Zircons can be separated in two main groups: magmatic and inherited. Magmatic zircons are relatively U-rich (average = 479 ppm) and have a pooled inverse concordia age of 350.3 ± 2.5 Ma (2σ, MSWD = 0.52, probability = 0.89, n = 8), Lower Mississippian, Tournaisian (Figs. 15 and 16). The sample has a population of inherited zircon with a mean average of $^{206}Pb/^{238}U$ ages at 477.1 ± 2.0 Ma (Lower Ordovician, Floian). Some of the zircons of this population may be metamorphic as indicated by the absence of zoning and the very low Th/U ratios of 0.039.

Sample LD (Mazán granite) has a population of large grains of zircon (about 200 μm long), which are significantly fractured, inclusion-rich and partially metamict. Only a few grains have unaltered areas to be analyzed. Metamictization is explained by the high content in U (average is 975 ppm), whereas the Th content is low (52 ppm) as are the Th/U ratios (average is 0.057). It is interpreted that all zircons of this sample have crystallized during an Ordovician magmatic event (Fig. 17). The age of this magmatic event is 471 ± 5 Ma (MSWD = 0.28, probability = 0.60, at 2σ, n = 9), which is within error of the age of the inherited zircon of sample CN19 (477 ± 2 Ma).

Sample SM13 (La Quebrada granite) is zircon-poor and only 20 grains were recovered from the sample preparation process. Among these 20 grains some are too small to be analyzed (<20 μm), whereas others are too poor in U (<20 ppm). Only eight acceptable analyses were obtained. The content in radiogenic Pb is very low (<10 ppm) and the amount of ^{207}Pb is minimal (<0.5 ppm). This fact impedes using the concordia plots and the calculated age is a mean average of the $^{206}Pb/^{238}U$ ages: 352.3 ± 3.9 Ma (MSWD = 2.6, 2σ). This value corresponds to the Lower Mississippian, Tournaisian (Fig. 18).

6. Discussion

All of the studied granitoids in the western Sierras Pampeanas can be considered specialized granites (cf. Tischendorf, 1977; Table 1). They are unaltered peraluminous granites (Fig. 5). The undeformed

Table 4
U–Pb–Th SHRIMP data on zircons of selected samples from granitoids in the Sierras Pampeanas orogen, northwestern Argentina.

						Ratios					Ages		
	U	Th	Th	^{206}Pb	4f^{206}	^{207}Pb	^{207}Pb	^{206}Pb	Error	^{208}Pb	^{206}Pb	^{206}Pb	Disc.
Spot	ppm	ppm	U	ppm	%	^{206}Pb	^{235}U	^{238}U	Correl.	^{232}Th	^{238}U	^{207}Pb	%
LD, Mazán barren granite (La Descubridora zone)													
a.3-1	935	26	0.03	62.2	0.12	0.05577 ± 1.73	0.5953 ± 2.06	0.0774 ± 1.12	0.545	0.0160 ± 27.21	480.7 ± 5.2	443 ± 38	−8
a.4-1	700	41	0.06	45.2	0.05	0.05632 ± 1.49	0.5827 ± 1.88	0.0750 ± 1.15	0.611	0.0226 ± 7.39	466.4 ± 5.2	465 ± 33	0
a.5-1	789	48	0.06	52.2	−0.03	0.05724 ± 1.09	0.6075 ± 1.58	0.0770 ± 1.13	0.720	0.0257 ± 3.49	478.1 ± 5.2	501 ± 24	5
a.6-1	1059	58	0.06	68.0	0.02	0.05773 ± 1.05	0.5949 ± 1.53	0.0747 ± 1.12	0.727	0.0221 ± 4.67	464.6 ± 5.0	520 ± 23	11
a.7-1	924	69	0.08	60.5	0.09	0.05595 ± 1.23	0.5878 ± 1.68	0.0762 ± 1.15	0.683	0.0220 ± 5.02	473.4 ± 5.2	450 ± 27	−5
a.10-1	887	63	0.07	58.9	0.01	0.05610 ± 1.21	0.5980 ± 1.66	0.0773 ± 1.13	0.680	0.0232 ± 4.90	480.0 ± 5.2	456 ± 27	−5
a.11-1	1336	55	0.04	87.2	0.08	0.05722 ± 0.83	0.5987 ± 1.43	0.0759 ± 1.17	0.815	0.0241 ± 6.38	471.5 ± 5.3	500 ± 18	6
a.13-1	910	77	0.09	58.8	0.62	0.05668 ± 1.79	0.5841 ± 2.16	0.0747 ± 1.22	0.564	0.0207 ± 10.82	464.7 ± 5.5	479 ± 39	3
a.14-1	1235	30	0.02	78.8	0.00	0.05561 ± 0.90	0.5694 ± 1.38	0.0743 ± 1.04	0.755	0.0231 ± 3.50	461.8 ± 4.6	437 ± 20	−6
SM13, La Quebrada Granite													
e.2-1	197	109	0.57	9.6	−0.15	0.05607 ± 3.08	0.4380 ± 3.34	0.0567 ± 1.28	0.384	0.0178 ± 2.84	355.3 ± 4.4	455 ± 68	22
e.2-2	198	138	0.72	9.4	0.04	0.05337 ± 2.92	0.4096 ± 3.16	0.0557 ± 1.29	0.401	0.0171 ± 2.54	349.2 ± 4.3	345 ± 65	−1
e.3-1	95	326	3.56	4.6	0.30	0.04882 ± 5.01	0.3772 ± 5.34	0.0560 ± 1.85	0.347	0.0168 ± 2.40	351.5 ± 6.3	139 ± 118	−152
e.3-2	132	131	1.03	6.5	0.18	0.05214 ± 8.63	0.3772 ± 5.34	0.0560 ± 1.85	0.347	0.0168 ± 2.40	357.8 ± 5.2	293 ± 193	−22
e.4-1	56	202	3.75	2.6	−1.45	0.07093 ± 3.75	0.5458 ± 4.41	0.0558 ± 2.32	0.526	0.0197 ± 2.84	350.1 ± 7.9	955 ± 77	63
e.6-1	116	201	1.79	5.2	0.01	0.06238 ± 5.74	0.4946 ± 6.19	0.0575 ± 2.31	0.374	0.0172 ± 3.58	360.4 ± 4.9	687 ± 122	48
e.7-1	116	201	1.79	5.2	0.01	0.05722 ± 3.61	0.4132 ± 3.91	0.0524 ± 1.52	0.388	0.0169 ± 2.31	329.1 ± 4.9	500 ± 79	31
e.7-2	128	314	2.54	6.0	0.00	0.06145 ± 2.48	0.4690 ± 3.02	0.0554 ± 1.71	0.567	0.0174 ± 2.20	347.3 ± 5.8	655 ± 53	47
CN19, Cerro Colorado Granite													
d.1-1	1603	26	0.02	105.3	0.03	0.05608 ± 0.70	0.5913 ± 1.13	0.0765 ± 0.89	0.787	0.0233 ± 6.1	475.0 ± 4.1	455 ± 15	−4
d.1-2	315	30	0.10	20.9	0.07	0.05627 ± 1.50	0.5477 ± 2.65	0.0772 ± 1.09	0.381	0.0225 ± 10.50	479.7 ± 4.9	403 ± 59	−19
d.2-1	428	167	0.40	20.5	0.30	0.05303 ± 2.21	0.4070 ± 2.43	0.0557 ± 1.01	0.414	0.0172 ± 2.5	349.2 ± 3.4	330 ± 50	−6
d.2-2	157	145	0.95	7.6	0.24	0.05339 ± 3.36	0.4130 ± 3.58	0.0561 ± 1.23	0.344	0.0175 ± 2.2	351.9 ± 4.2	346 ± 76	−2
d.2-3	77	184	2.48	3.7	0.60	0.05502 ± 5.31	0.4263 ± 5.56	0.0562 ± 1.68	0.301	0.0177 ± 2.5	352.4 ± 5.7	413 ± 119	15
d.3-1	407	24	0.06	26.8	0.06	0.05584 ± 1.50	0.5893 ± 1.80	0.0765 ± 0.99	0.552	0.0249 ± 5.7	475.4 ± 4.6	446 ± 33	−7
d.3-2	563	68	0.13	27.6	0.69	0.05309 ± 3.33	0.4155 ± 3.47	0.0568 ± 0.99	0.284	0.0174 ± 11.4	355.9 ± 3.4	333 ± 76	−7
d.4-1	539	196	0.38	23.2	0.69	0.05299 ± 3.85	0.3643 ± 4.00	0.0499 ± 1.06	0.265	0.0167 ± 4.2	313.7 ± 3.2	329 ± 87	5
d.4-2	433	52	0.12	28.9	0.11	0.05608 ± 1.91	0.5999 ± 2.17	0.0775 ± 1.04	0.478	0.0243 ± 5.5	481.3 ± 4.8	457 ± 42	−5
d.4-3	393	29	0.08	24.9	0.00	0.05820 ± 1.42	0.5918 ± 1.80	0.0737 ± 1.10	0.614	0.0255 ± 3.8	458.7 ± 4.9	537 ± 31	15
d.4-4	450	174	0.40	21.4	0.80	0.05481 ± 3.29	0.4151 ± 3.48	0.0549 ± 1.15	0.329	0.0169 ± 4.1	344.7 ± 3.9	404 ± 74	15
d.5-1	132	242	1.89	6.4	0.36	0.05381 ± 3.56	0.4168 ± 3.79	0.0562 ± 1.31	0.345	0.0175 ± 2.4	352.3 ± 4.5	363 ± 80	3
d.5-2	142	159	1.15	6.7	0.01	0.05339 ± 4.41	0.4027 ± 4.63	0.0547 ± 1.41	0.304	0.0181 ± 2.5	343.3 ± 4.7	346 ± 100	1
d.5-3	81	136	1.74	4.0	1.59	0.05253 ± 10.8	0.4085 ± 11.0	0.0564 ± 1.97	0.179	0.0172 ± 3.8	353.7 ± 6.8	309 ± 247	−15
d.6-1	684	87	0.13	45.4	0.05	0.05644 ± 1.16	0.6011 ± 1.54	0.0772 ± 1.01	0.657	0.0239 ± 3.1	479.6 ± 4.7	470 ± 26	−2

Notes: Isotopic ratios errors in%
All Pb in ratios are radiogenic component corrected using ^{204}Pb content.
disc. = discordance, as 100–100{t[^{206}Pb/^{238}U]/t[^{207}Pb/^{206}Pb]}
f206 = (common ^{206}Pb)/(total measured ^{206}Pb) based on measured ^{204}Pb.
Uncertainties are 1σ.

Carboniferous granite stocks from the Sierras de Velasco, Mazán, Ancasti and Cerro Negro, can be classified as late to post-tectonic granites (cf. Báez, 2006; Fogliata, 1999; Toselli et al., 1983).

In this paper, we used Rb, Sr, Ba, Li, Zr and Th, as pathfinder elements as proposed by Olade (1980), who used them to define mineralized Sn–W and barren granites in the north of Nigeria. In the granites of the western Sierras Pampeanas, there is a distinct enrichment of Rb and Li and depletion of Ba and Sr in the mineralized granites. This is reflected in Figs. 10 and 13 using the ternary Rb–Ba–Sr diagram by El Bousely and El Sokkary (1975) and GCI by Srivastava and Sinha (1997), respectively.

The total contents of REE <100 ppm may be due to fractionation of accessory minerals such as apatite and zircon, and/or mobilization of REE through complex Cl-REE and F-REE in late post-magmatic fluids (Irber, 1999; Taylor et al., 1981). The total contents of granites with REE of <100 ppm correspond to the most evolved and related mineralization such as the Carboniferous granites of the Central Iberian Zone with Sn and W associated mineralization (Ruiz et al., 2008). The ratio La_N/Lu_N reflects the degree of REE fractionation with the lowest values compatible with low total REE contents. The Sn–W bearing granites in the study area are characterized by low La_N/Lu_N ratios.

Using conventional U–Pb, SHRIMP and Rb–Sr dating reveals that all the studied granites in the Sierras Pampeanas crystallized in the Tremadocian–Carboniferous. The El Durazno granite was not dated but intruded the Antinaco orthogneiss and is undeformed. Both of these characteristics are common for Carboniferous granites of the Sierra de Velasco. Therefore, the El Durazno granite is likely to be the same age as the San Blas granitoid (i.e., 334 ± 5 Ma; Báez et al., 2004). However, the Cerro Colorado and La Quebrada granite stocks contain inherited zircons that point towards a metamorphic environment (based on absence of zoning, low Th and Th/U ratios) during crystallization. Those zircons yielded Floian (Lower-Ordovician) ages, which are consistent with regional metamorphism during the Ordovician in the Sierras Pampeanas.

Based on our study, there is a distinct relationship between Carboniferous magmatism and Sn–W mineralizations in the western Sierras Pampeanas. The Sn–W mineralization in the western Sierras Pampeanas is related to granitic magmas with significant crustal component, emplaced at a high crustal level in an extensional environment during the Late Devonian–Early Carboniferous, significantly after the compressive deformation that characterizes the country rocks. The new geochronological data presented here is compatible with observations by Fogliata et al. (2008), who propose that the

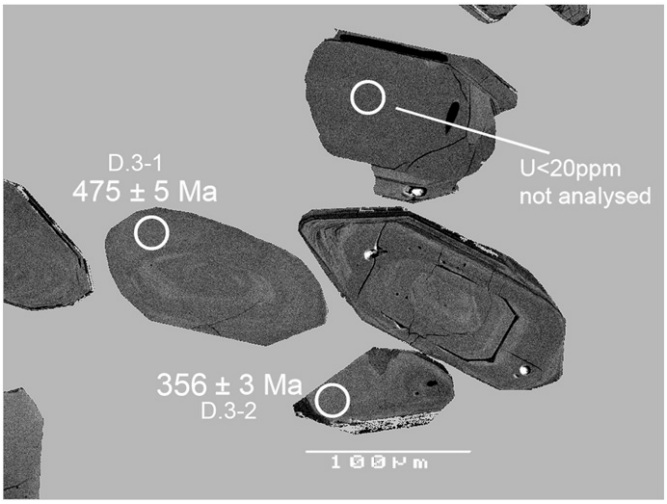

Fig. 15. Back-scattered electron image of zircons in sample CN19 showing the locations of the analytical spots (white circles) and the $^{206}Pb/^{238}U$ ages.

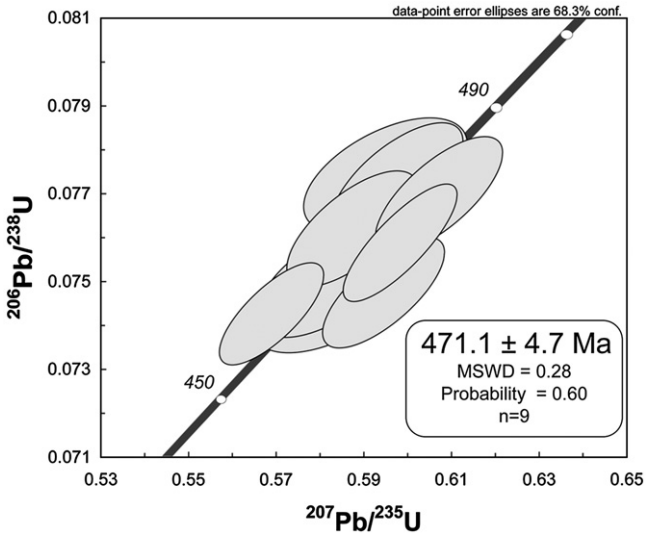

Fig. 17. SHRIMP conchordia plots for zircons in geochronological sample LD (Mazán barren granite).

Carboniferous magmatism W as the main metallogenic control in the western Sierras Pampeanas. This marks a difference from granites that are associated with Sn–W mineralization in the Eastern Tin belt of Bolivia, which are Late Permian (Arce-Burgot and Goldfarb, 2009). Other worldwide examples of Carboniferous granites that are associated with Sn–W mineralization include the leucogranites of the Jalama batholiths in the central Iberian zone (Ruiz et al., 2008).

7. Conclusions

The geochemical and geochronological investigations on the San Blas, Huaco and El Durazo granite stocks from the Sierra de Velasco, the La Quebrada granite from the Sierra de Mazán, Cerro Colorado from the Cerro Negro, and Mudaderos and Sauce Guacho granite stocks from the Sierra de Ancasti, in the western Sierras Pampeanas have revealed the following:

1. The majority of the studied granites are peraluminous (ASI between 1.05 and 1.38). They represent S-type granites emplaced in an extensional regime.
2. Based on total alkalis versus silica, all the studied samples represent Sn- and W-bearing granites.
3. The undeformed and unaltered granite stocks in the Sierras Velasco, Mazán, Ancasti and Cerro Negro are late to post-tectonic granites.
4. Mineralized granites display higher values in Sn and Rb, and lower values in Sr and lower values of Ba compared to barren granites.
5. The geochemical characterization index (GCI), confirms known mineralized and barren granites in the Sierras Pampeanas. In the Sierra de Ancasti granite, there is presently no known associated Sn–W mineralization but GCI values from samples indicate that it is highly prospective.
6. All the sampled granites display elevated values of LREEs, low values of HREE and negative Eu anomalies. In terms of total REEs values, the studied granite can be subdivided into two groups: (1) the Huaco, Cerro Colorado, the granular facies of the San Blas and Mudadero granite, which have a total REE of >100 ppm; and (2) aplite facies of the San Blas, El Durazno, and La Quebrada and Sauce Guacho, which have a total REE of <100 ppm. The lower REE contents could be due to fractionation of accessory minerals and/or the mobilization of REE to late post-magmatic fluids. The second group represents highly evolved granites (i.e., high Rb/Sr ratios). This REE behavior is characteristic of Carboniferous Sn–W granites in the western Sierras Pampeanas.

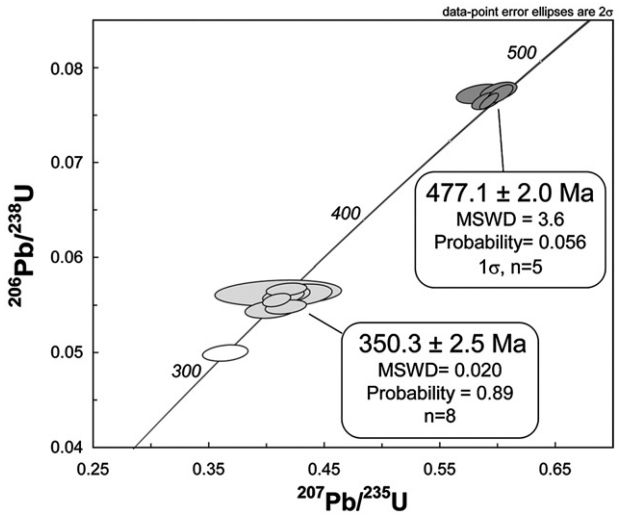

Fig. 16. SHRIMP conchordia plots for zircons in geochronological sample CN19.

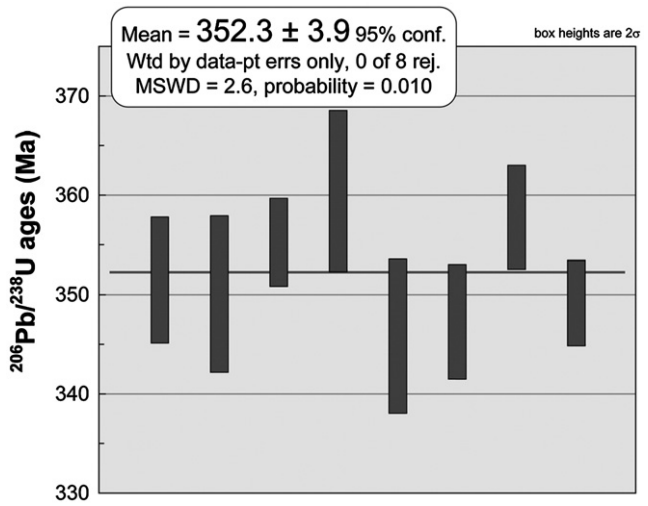

Fig. 18. Calculated age from zircons in geochronological sample SM13.

7. The new geochronological data from the Cerro Colorado and the La Quebrada granites support the idea that Sn–W mineralization in the western Sierras Pampeanas is related to evolved Carboniferous granites.
8. The Carboniferous contains significant Sn–W mineralization in the western Sierras Pampeanas, which is in contrast to the Late Permian Sn–W mineralization in the Eastern Tin belt of Bolivia. Therefore, the western Sierras Pampeanas is not simply the southern geological extension of the latter.

Acknowledgments

The authors gratefully acknowledge the financial and in-kind support from Fundación Miguel Lillo, the National University of Tucumán, and the Centre for Exploration Targeting at the University of Western Australia. We also appreciate the cooperation of Juan Ryziuk and. Sebastian Espinosa. Christian Schindler is thanked for assisting in creating diagrams and tables. Particular thanks to Iris Sonntag for critically reading an earlier version of this manuscript. We also much appreciate the detailed reviews by Wally Witt, John Carranza and an anonymous reviewer.

References

Amos, A., Zardini, R., 1962. Geología de algunos depósitos de arcilla de La Rioja. Rev. Asoc. Geol. Argent. 17, 47–83.
Anders, E., Grevesse, N., 1989. Abundances of the elements: meteoritic and solar. Geochim. Cosmochim. Acta 53, 197–214.
Arce-Burgot, O., Goldfarb, R., 2009. Metallogeny of Bolivia. SEG Newsl. 79, 8–15.
Báez, M.A., 2006. Geología, Petrografía y Geoquímica del Basamento Ígneo Metamórfico del sector norte de la Sierra de Velasco, provincia de la Rioja. Tesis Doctoral. Facultad de Ciencias Exactas, Físicas y Naturales de la Universidad Nacional de Córdoba, 207 pp.
Báez, M., Basei, M.A., Toselli, A.J., Rossi, J., 2004. Geocronología de granitos de la sierra de Velasco (Argentina): reinterpretación de la secuencia magmática. Simposio Quarenta Anos de Geocronologia no Brasil (CPGeo). Universidade de São Paulo (USP) Actas, p. 85.
Báez, M., Bellos, L., Grosse, P., Sardi, F.G., 2005. Caracterización petrológica de la sierra de Velasco. In: Dahlquist, J., Rapela, C., Baldo, E. (Eds.), Geología de la provincia de La Rioja -Precámbrico-Paleozoico Inferior: Asociación Geológica Argentina, Serie D, Publicación especial Nº 8, pp. 123–130.
Baker, T., Pollard, P., Mustard, R., Mark, G., Grahan, J., 2005. A comparison of granite-related tin, tungsten and gold–bismuth deposits: implications for exploration. SEG Newsl. 61, 9–17.
Bellos, L., Grosse, P., Ruíz, A., Rossi, J.N., Toselli, A., 2002. Petrografía y geoquímica de granitoides del flanco sud-occidental de la sierra de Velasco, La Rioja, Argentina: XV Congreso Geológico Argentino, Calafate, 2, pp. 81–86.
Bossi, G.E., Sanagua, J., Georgieff, S., Ibáñez, L., Muruaga, C., Quiroga, G., 1996. Discordancias sinsedimentarias en conglomerados de pie de monte del extremo norte de la sierra de Velasco, La Rioja, Argentina. Actas Reunión Argentina de Sedimentología, Bahía Blanca, p. 16.
Compston, W., Williams, I.S., Kirschvink, J.L., Zichao, Z., Guogan, M., 1992. Zircon ages for the Early Cambrian timescale. J. Geol. Soc. Lond. 149, 171–184.
Cravero, O. 1983. Manifestación estannifera "Casa Pintada". Dirección de Nacional de Geología y Minería, Plan La Rioja. Informe Nº 182 (inédito), 3 pp.
Dahlquist, J.A., Pankhurst, R., Rapela, C.W., Casquet, C., Fanning, C.M., Alasino, P.H., Báez, M., 2006. The San Blas Pluton: an example of the Carboniferous plutonism in the Sierras Pampeanas, Argentina. J. South Am. Earth Sci. 20, 341–350.
Dall Agnol, R., Lafon, J.M., Macambira, M.J.B., 1994. Proterozoic and orogenic magmatism in the Central Amazonian Province, Amazonian Craton: geochronological, petrological and geochemical aspects. Mineral. Petrol. 50, 113–138.
De Alba, E., 1979. Descripción geológica de la Hoja 16 d "Chilecito" (provincia de La Rioja). Dirección Nacional de Minería y Geología; boletín Nº 163.
De Laeter, J.R., Kennedy, A.K., 1998. A double focusing mass spectrometer for geochronology. Int. J. Mass Spectrom. 178, 43–50.
El Bousely, A.M., El Sokkary, A.A., 1975. The relation between Rb, Ba and Sr in granitic rocks. Chem. Geol. 16, 207–219.
Fogliata, A.S., 1999. Estudio geológico económico de los recursos mineros de la Sierra de Mazán. Tesis Doctoral. Facultad de Ciencias Naturales e Instituto M. Lillo, Universidad Nacional de Tucumán, 203 pp.
Fogliata, A.S., Ávila, J., 1997. Manifestaciones minerales de la ladera occidental del cerro Mazán, provincia de La Rioja, Argentina. VIII Congreso Geológico Chileno. Antofagasta, Chile II, pp. 961–965.
Fogliata, A.S., Ávila, J., 2001. Caracterización del greisen asociado a depósitos de estaño y wolframio paleozoicos, Sierra de Mazán (La Rioja, Argentina). Boletín Geológico y Minero de España 112-1, pp. 19–32.
Fogliata, A., Báez, M., 2008. Estudio comparativo del efecto tetrada en tierras raras entre los granitos La Quebrada, sierra de y San Blas, sierra de Velasco, La Rioja: 9° Congreso de Mineralogía y Metalogenia. San Salvador de Jujuy, 1, pp. 185–188.
Fogliata, A., Mas, G., Ávila, J.C., 1998. Las wolframitas de Mazán, La Rioja: caracteres mineralógicos y composicionales: IV Reunión de Mineralogía y Metalogénesis, 1, pp. 77–82.
Fogliata, A., Rubinstein, N., Ávila, J., Báez, M., 2008. Depósitos de greisen asociados a granitos carboníferos post-orogénicos con potencial mineralizador, Sierra de Fiambalá, Catamarca, Argentina: Boletín Geológico y Minero de España, 119, pp. 509–524.
González Bonorino, F., 1950. Algunos problemas geológicos de las sierras Pampeanas. Rev. Asoc. Geol. Argent. 5, 81–110.
González Bonorino, F., 1951. Una nueva Formación precámbrica en el Noroeste Argentino. Comunicaciones Científicas Museo 5.
Grosse, P., Sardi, F., 2005. Geología de los granitos Huaco y Sanagasta, sector centro-oriental de la Sierra de Velasco, La Rioja: Simposio Bodenbender, Serie de Correlación Geológica (INSUGEO), 19, pp. 221–238.
Grosse, P., Sollner, F., Báez, M., Toselli, A., Rossi, J., De La Rosa, J.D., 2009. Lower Carboniferous post-orogenic granites in central-eastern Sierra de Velasco, Sierras Pampeanas, Argentina: U–Pb monazite geochronology, geochemistry and Sr–Nd isotopes. Int. J. Earth Sci. 98, 1001–1025.
Irber, W., 1999. The lanthanide tetrad effect and its correlation with K/Rb, Eu/Eu*, Sr/Eu, Y/Ho and Zr/Hf of evolving peraluminous granite suites. Geochim. Cosmochim. Acta 63 (3–4), 489–508.
Kamilli, R., Criss, R., 1996. Genesis of the Sisilah tin deposit, Kingdom of Saudi Arabia. Econ. Geol. 91, 1414–1434.
Kempe, U., Wolf, D., 2006. Anomalously high Sc contents in ore minerals from Sn–W deposits: possible economic significance and genetic implications. Ore Geol. Rev. 28, 103–122.
Knüver, M., 1983. Dataciones radimétricas de rocas plutónicas y metamórficas. In: Aceñolaza, Miller, Toselli (Eds.), La Geología de la sierra de Ancasti: Münster. Forsch. Geol. Paläont. . 372 pp.
Krauskopf, K., 1979. Introduction to Geochemistry, 2nd Ed. McGraw Hill Internat. Book. Company. 617 pp.
A Classification of Igneous Rocks and Glossary of Terms. In: Le Maitre, R.W. (Ed.), Blackwell Scientific Publications, Oxford.
Levinson, A.A., 1974. Introduction to Exploration Geochemistry. Applied Pub, Calgary (c1989, 612 pp.).
Linnen, R.N., 1998. Depth of emplacement, fluid provenance and metallogeny in granitic terranes: a comparison of western Thailand with other tin belts. Miner. Deposita 33, 461–476.
Ludwig, K.R., 1999. Using ISOPLOT/Ex, version 2: a geochronological toolkit for microsoft excel. Berkeley Geochronological Center Special Publication Ia. 47 pp.
Ludwig, K.R., 2002. Squid 1.02, user's manual: Berkeley Geochronological Center Special Publication, 2 (Berkeley, California, USA), 21 pp.
Maniar, P., Piccoli, P., 1989. Tectonic discrimination of granitoids. Bull. Geol. Soc. Am. 101, 635–643.
Martínez, L., 1978. Geología del área de Cerro Negro, departamento Tinogasta, provincia de Catamarca. Trabajo Final de Seminario, facultad de Ciencias Naturales e I.M.L, U.N.T. (Inédito) 46 pp.
Monecke, T., Kempe, U., Monecke, J., Sala, M., Wolf, D., 2002. Tetrad effect in rare earth element distribution patterns: a method of quantification with application to rock and mineral samples from granite-related rare metal deposits. Geochim. Cosmochim. Acta 66–7, 1185–1196.
Olade, M.A., 1980. Geochemical characteristics of tin bearing and tin-barren granites, Northern Nigeria. Econ. Geol. 75, 71–82.
Pollard, P.J., Pichavant, M., Charoy, V., 1987. Contrasting evolution of fluorine and boron-rich tin systems. Miner. Deposita 22, 315–321.
Ramos, V., 1999. Las provincias geológicas del territorio argentino. In: Caminos, R. (Ed.), Geología Argentina, Instituto de Geología y Recursos Minerales, Servicio geológico Minero Argentino: Anales, 29, pp. 41–96.
Ruiz, C., Fernández Lima, C., Locutora, J., 2008. Geochemistry, geochronology and mineralization potencial of the granites in the Central Zone: The Jalama batholith. Chem. Erde Geochem. 68, 413–429.
Sardi, F.G., 2005. Petrografía y caracterización de la mena del distrito pegmatítico Velasco, La Rioja, Argentina. XVI Congreso Geológico Argentino, La Plata V, pp. 231–238.
Söllner, F., Gerdes, A., Grosse, P., Toselli, A.J., 2007. U–Pb age determinations by LA-ICP-MS on zircons of the Huaco granite, Sierra de Velasco (NW-Argentina): a long-term history of melt activity within an igneous body. XX Colloquium on Latin American Earth Sciences, Kiel, Alemania, pp. 57–58.
Srivastava, P.K., Sinha, A.K., 1997. Geochemical characterization of tungsten-bearing granites from Rajasthan, India. J. Geochem. Explor. 60, 173–184.
Stipanicic, P., Linares, E., 1975. Catálogo de edades radimétricas determinadas para la República Argentina I: años 1960-1974. Rev. Asoc. Geol. Argent. Serie B 3–42.
Takahashi, Y., Yoshida, H., Sato, N., Hama, K., Yusa, Y., Shimizu, H., 2002. W- and M-Type tetrad effects in REE patterns for water-rock systems in the Tono uranium deposit, Central Japan. Chem. Geol. 184, 311–335.
Tauson, L.V., Kozlov, V.D., 1973. Distribution functions and ratios of trace elements, concentrations as estimates of ore bearing potencial of granites, in Geochemical Exploration 1977. Institute of Mining Metallurgy, London, pp. 37–44.
Taylor, R.P., Strong, D.F., Fryer, B.J., 1981. Volatile control of contrasting trace element distribution in peralkaline granitic and volcanic rocks. Contrib. Mineral. Petrol. 77, 267–271.
Thirlwall, M.F., Jenkins, C., Vroon, P.Z., Mattey, D.P., 1997. Crustal interaction during construction of ocean islands: Pb–Sr–Nd–O isotope geochemistry of the shield basalts of Gran Canaria, Canary Islands. Chem. Geol. 135 (3–4), 233–262.

Tischendorf, G., 1977. Geological and petrographic characteristics of silicic magmatic rocks with rare element mineralization. In: Stemprok, M., Burnol, L., Tischendorf, G. (Eds.), Metallization associated with acid magmatism: Geological Survey, 2, pp. 41–96.

Toselli, A.J., Rossi de Toselli, J., 1986. A proposal for the systematization of the Upper Precambrian–Lower Paleozoic basement in the Sierras Pampeanas, Argentina. Zentralbl. Geol. Palaeontol. Teil 1 9, 1227–1233.

Toselli, G., Toselli, A.J., 1990. Deformación dúctil en los granitoides de la sierra de Mazán, La Rioja, Argentina: XI Congreso Geológico Argentino, 5, pp. 147–177.

Toselli, J., Reissinger, M., Durand, F., Bazán, C., 1983. Rocas graníticas. In: Aceñolaza, Miller, Toselli (Eds.), La Geología de la sierra de Ancasti: Münster. Forsch. Geol. Paläont. 372 pp.

Verdecchia, S., Baldo, E., Benedetto, J., Borghi, P., 2007. The first shelly fauna from metamorphic rocks of the Sierras Pampeanas (La Cébila Formation, Sierra de Ambato, Argentina): age and paleogeographic implications. Ameghiniana 44, 493–498.

Vriend, S.P., Oosterom, M.G., Bussink, R.W., Jansen, J.B.H., 1985. Trace-element behavior of the W–Sn granite of Regoufe, Portugal. J. Geochem. Explor. 23, 13–25.

Xie, L., Wang, R., Chen, J., Zhu, J., Zhang, W., Wang, D., Yu, A., 2009. Primary Sn-rich titanite in the Qitianling granite, Hunan Province, southern exploration. China Sci. Bull. 54, 798–805.